Technical Note N-1362

EVALUATION OF HYDROACOUSTIC RAPID-IMPACTING PILE DRIVER

by

Carter J. Ward, Ph.D.

November 1974

Sponsored by
NAVAL FACILITIES ENGINEERING COMMAND

Approved for public release; distribution unlimited.

CIVIL ENGINEERING LABORATORY
Naval Construction Battalion Center
Port Hueneme, California 93043

Unclassified

SECURITY CLASSIFICATION OF THIS PAGE *(When Data Entered)*

REPORT DOCUMENTATION PAGE		READ INSTRUCTIONS BEFORE COMPLETING FORM
1. REPORT NUMBER TN-1362	2. GOVT ACCESSION NO. DN244024	3. RECIPIENT'S CATALOG NUMBER
4. TITLE *(and Subtitle)* EVALUATION OF HYDROACOUSTIC RAPID-IMPACTING PILE DRIVER		5. TYPE OF REPORT & PERIOD COVERED Final; 1 July 1971—30 Jun 1973 6. PERFORMING ORG. REPORT NUMBER
7. AUTHOR*(s)* Carter J. Ward, Ph.D.		8. CONTRACT OR GRANT NUMBER*(s)*
9. PERFORMING ORGANIZATION NAME AND ADDRESS CIVIL ENGINEERING LABORATORY Naval Construction Battalion Center Port Hueneme, California 93043		10. PROGRAM ELEMENT, PROJECT, TASK AREA & WORK UNIT NUMBERS 62755N YF53.536.006.01.011
11. CONTROLLING OFFICE NAME AND ADDRESS Naval Facilities Engineering Command Alexandria, Virginia 22332		12. REPORT DATE November 1974 13. NUMBER OF PAGES 46
14. MONITORING AGENCY NAME & ADDRESS*(if different from Controlling Office)*		15. SECURITY CLASS. *(of this report)* Unclassified 15a. DECLASSIFICATION DOWNGRADING SCHEDULE

16. DISTRIBUTION STATEMENT *(of this Report)*

Approved for public release; distribution unlimited.

17. DISTRIBUTION STATEMENT *(of the abstract entered in Block 20, if different from Report)*

18. SUPPLEMENTARY NOTES

19. KEY WORDS *(Continue on reverse side if necessary and identify by block number)*

Hydroacoustic impact tool, hydroacoustic driver, hydroacoustic pile driver, pile driver, rapid-impacting pile driver.

20. ABSTRACT *(Continue on reverse side if necessary and identify by block number)*

Tests to evaluate the driving capabilities of the rapid-impacting hydroacoustic pile driver on various types and sizes of vertical piles and horizontal batter piles are described and discussed. The functional and operational characteristics of the driver are described, test results and output analysis are presented, and the hydroacoustic driver is compared operationally and economically with the vibratory driver and conventional diesel pile hammer.

DD FORM 1 JAN 73 1473 EDITION OF 1 NOV 65 IS OBSOLETE

continued

Unclassified

SECURITY CLASSIFICATION OF THIS PAGE *(When Data Entered)*

20. Continued

Interpretation of the results indicates that the hydroacoustic driver is capable of rapidly driving vertical and batter piles at a rate of 30 feet per minute for wood and steel and 12 feet per minute for concrete. Diesel driving in similar soil by CEL averaged 2.5 feet per minute for wood and 1.6 feet per minute for concrete.

The hydroacoustic driver tested is an experimental model. Development of a full-scale prototype rapid-impacting hydroacoustic driver is required prior to Navy adoption.

CONTENTS

INTRODUCTION

Single-impact diesel hammers are currently used by the Navy for driving piles. Newly developed techniques, such as Bodine's sonic pile driver, rapid-impacting pile hammers, and other vibratory pile drivers may substantially improve upon current pile-driving methods [1,2]. Claims of greater efficiency have been made by commercial developers [3], and test results outlined in this report indicate that some of these claims are valid.

Diesel-powered single-impact hammers currently used by Seabees must in effect wait for the dynamic response of a blow to subside before the next blow can be made, while the rapid-impacting technique allows blows in rapid succession. In addition, the single-impact diesel hammer does not operate satisfactorily in very soft soils [4] because the hammer is unable to rebound under soft-soil conditions, and continuous operation ceases. It then must be hoisted and dropped by the crane for each individual blow, with this slow hoist and drop procedure continuing until sufficiently solid soil resistance is met. A study by the Michigan State Highway Commission of diesel pile hammers predicts some improvements, but these have not yet become fact [5]. The results of the Michigan study indicate that loss of 1/3 to 2/3 of the rated energy of diesel pile drivers occurs during impact, due to the cushioned drive cap mechanism for transmitting the energy to the pile.

General Dynamics, and subsequently Hydroacoustics Incorporated,* developed a prototype rapid-impacting pile driver that uses high-frequency hydraulic oscillators that permit the development of large amounts of impact energy from a comparatively small device [2]. It is capable of operation at high frequencies and can penetrate rock layers [6]. The hydroacoustic impact tool delivers compressive force pulses to the pile, driving it in one direction only; a vibratory driver on the other hand expends much of its energy by alternately inserting and withdrawing the pile, leading to high energy dissipation along the sides of the pile. It is expected that much less input power will be required for a hydroacoustic driver compared to a vibratory driver, with a consequent reduction in pile stresses [3]. The hydroacoustic pile driver is able to drive piles made of concrete or wood materials in addition to steel. It does not require a clamp to grip the pile, thus eliminating one of the more complex parts of a vibratory driver. The hydroacoustic driver can also operate in air or under water to drive and extract piles at a high rate in vertical as well as batter (inclined to the horizontal) positions.

*Hydroacoustics Inc. purchased patent rights from General Dynamics for the hydroacoustic driver.

DESCRIPTION OF HYDROACOUSTIC PILE DRIVER

The hydroacoustic oscillator is an entirely new hydraulically driven rapid-impacting pile driver. Figure 1 illustrates the principal features. The device contains a hydraulic oscillator that delivers energy by impacting an anvil. The energy rate is a function of the frequency and hammer impact velocity. The valve-hammer impacting mass separates two liquid-filled cavities, cavities 1 and 2 in Figure 1, and is freely supported in the cylinder. Oscillation is maintained by alternating pressures in the fluid cavities. As a result, the fluid-mass system forms a simple spring-mass oscillator with the liquid-filled cavities reacting as springs. Resonant frequency, f_o, is given below [7].

$$f_o = \frac{A_H}{2\pi}\sqrt{\frac{g_o B_F}{M_H}}\left(\frac{1}{V_1} + \frac{1}{V_2}\right) \tag{1}$$

where A_H = hammer cross-sectional area

g_o = conversion factor, 32.2 lbm-ft/lbf-sec^2

M_H = hammer mass

B_F = liquid bulk modulus (lbf/in.^{2})

V_1, V_2 = volume of cavities 1 and 2, respectively

An equivalent system would be that of a rigid mass suspended between two springs with spring constants equal to $(A_H^2 B_F/V_n)$, i.e.,

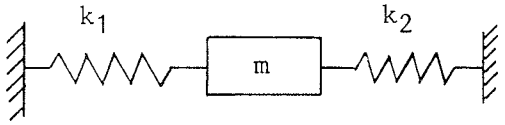

$$f = \frac{1}{2\pi}\sqrt{\frac{k_1}{m} + \frac{k_2}{m}} \tag{2}$$

One can see that the resonant frequency, f_o, may be altered by changing the oscillator mass or spring constant (i.e., fluid bulk modulus, hammer area, or cavity volume). One of the real advantages of a fluid oscillator is the high bulk modulus which enables a massive hammer to oscillate at a high frequency.

The oscillation is sustained by flow of pressurized hydraulic fluid through the device. Flow enters the top cavity, no. 1 in Figure 1, forcing the hammer down until the top reaches the return orifice. At this position the upper cavity pressure exhausts through the valve and the lower cavity pressure forces the hammer up for the cycle to repeat. It should be pointed out that the fluid must be compressible, otherwise it could not store the

energy needed to push the hammer up. As the hammer oscillates between its extreme positions, impact occurs on the anvil. By controlling the inlet flow, lower cavity pressure, and anvil dimensions, the pulse duration and force shape may be somewhat optimized. The word 'somewhat' is used here to indicate that the force shape is not totally controllable and that a well-defined optimum remains unknown. The pulse shape is examined in the discussion. The pulse duration of the hydroacoustic driver is longer than that of conventional percussion drills using impact [7]. This widening of the pulse shape allows a higher energy flow for a constant force. A duration of about 0.8 to 1.0 millisecond for the hydroacoustic oscillator was typical for the data recorded at CEL. Table 1 illustrates the operating characteristics extracted from the test data.

A photograph of the pile driver used during the test is shown in Figure 2. The hydroacoustic oscillator section of the tool consists of a cylindrical pressure vessel approximately 6 inches in diameter and 4 feet long, with its associated inlet and outlet plumbing. Above the oscillator section is a load yoke designed to receive the surcharge load. A downward force is applied on the axis of the oscillator section by a rod that bears on the top center of the oscillator end cap. The two tension cylinders at the sides of the yoke seen in Figure 2 are used for alignment when reloading a new pile. A split ring, shown in Figure 3, is welded onto the pile cap diameter below the shoulder and thus provides a means for the pulling yoke to apply an upward force against the pile cap and pile. After the new pile is properly aligned, the tension cylinders are loosened so that the total load is applied to the pile through the driver assembly.

Attached to the lower end of the oscillator is an adapter section approximately 10 inches in diameter and 1 foot long used for pipe piling. A short length of pipe pile was converted into a special adapter for driving the wood, concrete, and sheet piles. Impact is applied to the top end of the pile adapter and is transmitted to the pile through a shoulder which bears on top of the pile. The adapter section applies the surcharge static load from the oscillator housing to the top of the pile through the same shoulder. The static load used in the first test series was 6,000 pounds, dead weight. The second series used a hydrostatic winch which applied an average of 6,100 pounds.

TEST PROGRAM

The performance characteristics of the hydroacoustic rapid-impacting pile-driving hammer were compared with the diesel single-impact pile driving hammer of the type currently used by the Navy.* Hammer performance was analyzed using the factors of blowcount (blows per unit time), penetration rate, and energy delivered to the pile as comparison criteria. Tests were conducted with the prototype 4-inch pile-driving model to determine if the rapid impacts are equivalent to single impact or if significant favorable or unfavorable dynamic effects result.

---

* MKT Diesel Pile Hammer Models DE-20, DE-30 and DE-40.

Table 1. Test Results

Parameters	Pile Type					
	Steel Pipe (4" diam. x 20')	Steel Pipe (4" diam. x 40')	Concrete (8" diam. x 12' Tapered to 5-1/2" diam.)	Wood (3-1/2" x 3-1/2" x 16')	Wood (5-1/2" x 5-1/2" x 11')	Steel Sheet LBF – 1707 (18" x 12')
Surcharge, lb	6,000	6,000	6,200	6,000	6,000	6,600
Force duration, sec	0.008-0.001	0.0008	0.001	0.0008	0.0008	[a]
Penetration velocity, ft/sec	0.5	0.15-0.9	0.026-0.14	0.35-0.9	0.14-0.45	0.41-0.5
Max force, lb x 10^{-3}	15-25	11-16	26-35[b]	16-19[b]	18-28[b]	[a]
Energy per blow, ft-lb	25-75	8-27	75-130[b]	30-50[b]	50-100[b]	[a]
Upper cavity pressure, psi	3,000	2,950	2,500	3,000	3,000	2,300
Return pressure, psi	500	540	600	400	440	600
Lower cavity pressure, psi	1,700-2,300	2,400	1,700	1,600	1,600	1,700
Driver frequency, cps	125	125	122	125	125	[a]
Driver pressure drop, psi	2,500	2,410	1,900	1,600	1,560	1,700
Penetration per blow, in.	0.06-0.1	0.01-0.08	0.002-0.01	0.03-0.08	0.01-0.04	0.04-0.05
Driver flow rate, gpm	37-45	40	45	38	40	40-45

[a] Data not recorded.

[b] Data recorded on pile attachment.

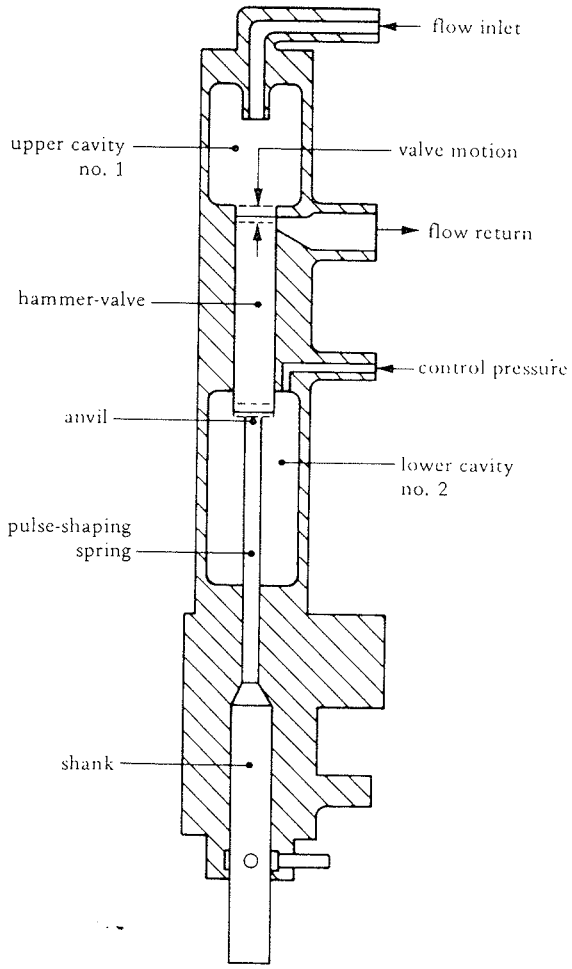

Figure 1. Hydroacoustic IMP III Rock Drill.

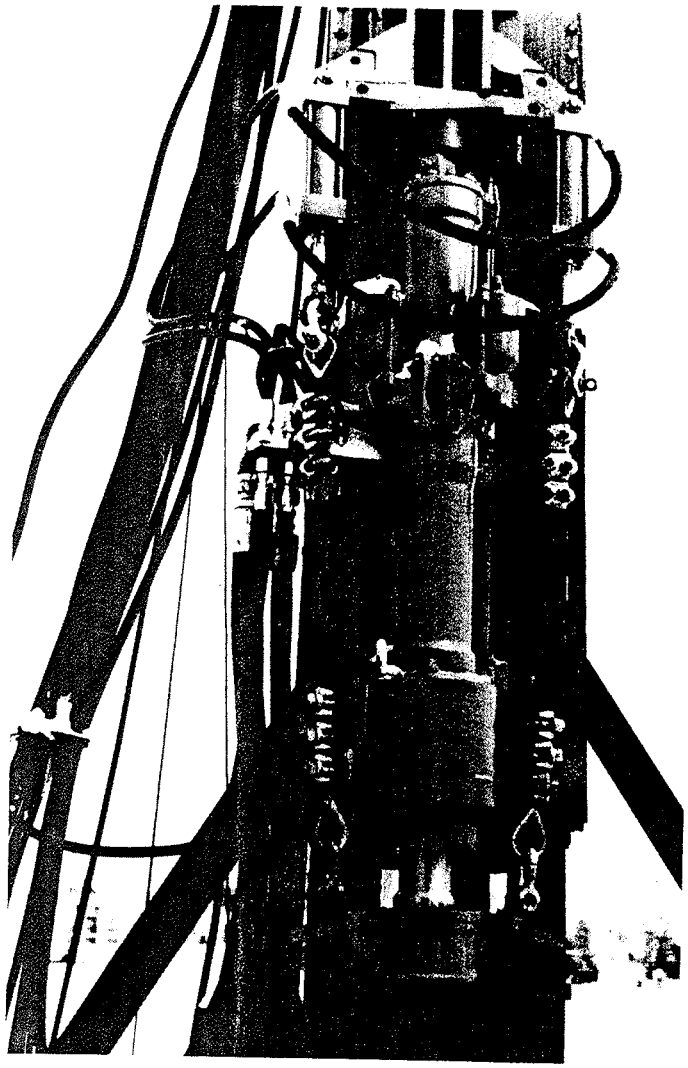

Figure 2. Prototype hydroacoustic pile driver.

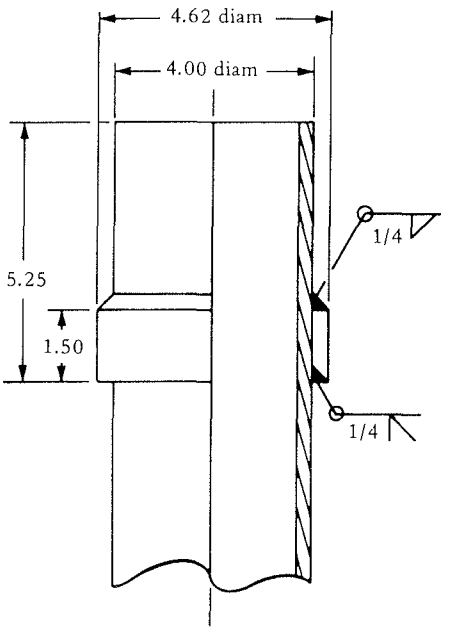

Figure 3. Pile pulling collar.

The individual tests conducted by CEL are listed below.*

1. Closed-end steel pipe piles 20 feet long and 4 inches, nominally, in diameter with a 5/16-inch wall thickness, were driven vertically to approximately 15 feet below the surface.

2. Closed-end steel pipe piles 40 feet long and 4 inches, nominally, in diameter with a 5/16-inch wall thickness, were driven vertically to approximately 25 feet below the surface.

3. Douglas fir posts, 3.5 inches by 3.5 inches by 12 feet long, were driven vertically to approximately 10 feet below the surface.

4. Douglas fir posts, 5.5 inches by 5.5 inches by 10 feet long, were driven vertically to approximately 8 feet below the surface.

5. Closed-end steel pipe piles (same as item 1 above) were driven in a batter position, inclined to the horizontal approximately 6 degrees, to a penetration depth of 15 feet. These tests drives were divided into two parts; half were driven into a bank of a dry excavation and half were driven with the pile and pile driver submerged approximately 2 feet under water in the excavation.

---

* Photographs of some of the tests are included in the Appendix.

6. Steel-reinforced concrete posts, 5 inches, nominally, in diameter and 12 feet long, were driven vertically to 10 feet below the surface.

7. Closed-end steel pipe piles (same as item 1) except for varying lengths, were driven vertically to depths of 8, 13, and 18 feet and tested for maximum bearing load capacity.

8. Foster type LBF-1707 steel sheet piles 12 feet long were driven vertically to 10 feet below the surface.

The instrumentation used to record each set of data are listed below.

Instrumentation

Longitudinal Strain. The dynamic longitudinal deflections were measured, using two strain gages mounted radially opposite each other with lead wires directly attached to the strain-gage instrumentation. Strain signals were observed continuously during driving. Figure 4 is a schematic of the instrumentation used. Note that the data required are high frequency in nature and that a common high pass filter arrangement was used to stabilize the circuit to obviate the need for a highly sensitive Wheatstone bridge. The circuit was calibrated with a known 125-cps sine wave voltage amplitude input.

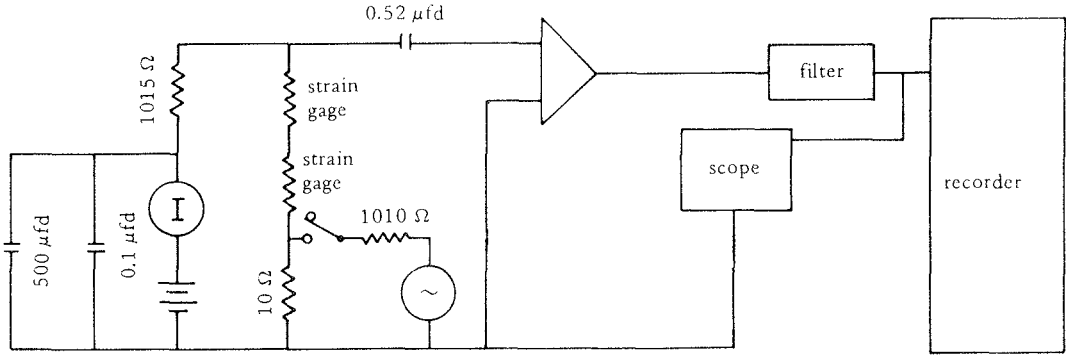

Figure 4. Instrumentation schematic.

Driving Velocity. The driving velocity was recorded in the first test series using a stop watch, by timing the penetration of known selected lengths of pile. In the second test series an audio tape recorder was used with a time base playback.

Hydraulic Flow Rate. This was measured with a venturi-type flowmeter in the control panel and was also checked with the flowmeter in the hydraulic power supply. Accuracy of the venturi meter was stated by the manufacturer to be in the range of ±5%.

Pressure Drop Across Oscillator. All pressures recorded were measured with standard Bourdon gages in the control panel, with gage lines connected to the points of interest. Equal-length gage lines were used for both input and output oscillator ports to eliminate the inequality of line pressure drops.

Energy Per Blow. The input energy per blow delivered to the pile was determined from the longitudinal strain pulse measured near the top of the pile. The relationship between the strain and energy may be derived from the longitudinal compression wave equation given below [8].

$$\frac{\partial^2 u}{\partial t^2} = \frac{E g_o}{\rho}\left(\frac{\partial^2 u}{\partial x^2}\right) \tag{3}$$

where u = displacement at the left face of the element dx (see Figure 5)

x = distance from reference fixed in space

dx = elemental length (see Figure 5)

ρ = density of rod material

t = time

g_o = conversion factor, 32.1739 lbm ft/sec^2 lbf

E = modulus of elasticity

∂ = partial derivative

A common solution, known as the characteristic solution, for u as a function of time may be derived from the preceding equation [9].

$$u = f(x - Ct) + f'(x + Ct) \tag{4}$$

where C = speed of sound in the rod material = $(E/\rho)^{1/2}$

f, f' = characteristic curve functions

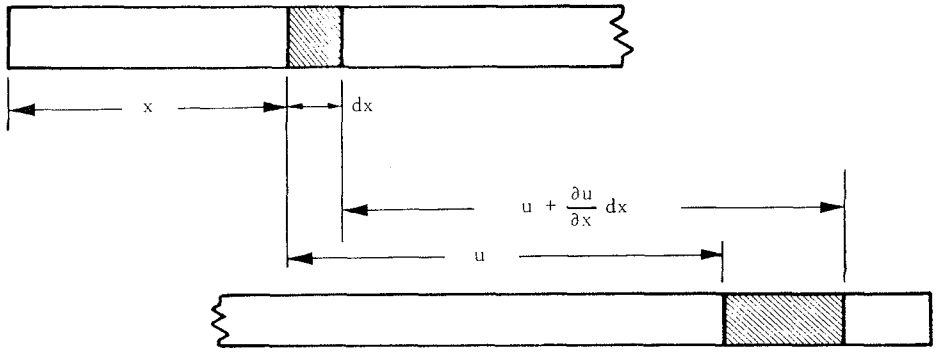

Figure 5. Element displacement due to longitudinal vibration in a uniform rod.

The velocity (V) of element dx, strain (ε), and stress (σ) of a point fixed in the element may then be obtained from the above function of u as follows:

$$V = \frac{\partial u}{\partial t}$$

$$\varepsilon = \frac{\partial u}{\partial x}$$

$$\sigma = E\varepsilon$$

From which the following relations are obtained.

$$\frac{V}{\sigma} = \frac{C}{E} \tag{5}$$

and with $C = (E/\rho)^{1/2}$,

$$V = \frac{\sigma}{\sqrt{E\rho}} \tag{6}$$

As a result, the energy per blow (K) may be determined [10].

$$K = \int_0^{u_o} F \, du$$

$$= \int_0^{t_o} F \frac{du}{dt} \, dt$$

$$= \int_0^{t_o} FV \, dt$$

$$= \int_0^{t_o} F \frac{\sigma}{\sqrt{E\rho}} \, dt$$

$$= \int_0^{t_o} \frac{F^2}{A\rho C} \, dt \qquad (7)$$

The force (F) is the product of stress and cross-sectional area and t_o is the pulse duration.

If the force shape as a function of time is assumed to be a clipped sine wave, the energy calculation is greatly simplified. The computation is relatively accurate for the pulse shapes produced by the hydroacoustic impact tool as may be seen in Figure 6. The resulting approximate energy per blow is:

$$K = \frac{1}{4\pi} \left[\frac{(F_{max})^2 \, t_o}{A\rho C} \right] \qquad (8)$$

It is interesting to note that the power flow through element dx is equal to the energy flow rate; i.e., number of blows per second times the energy per blow.

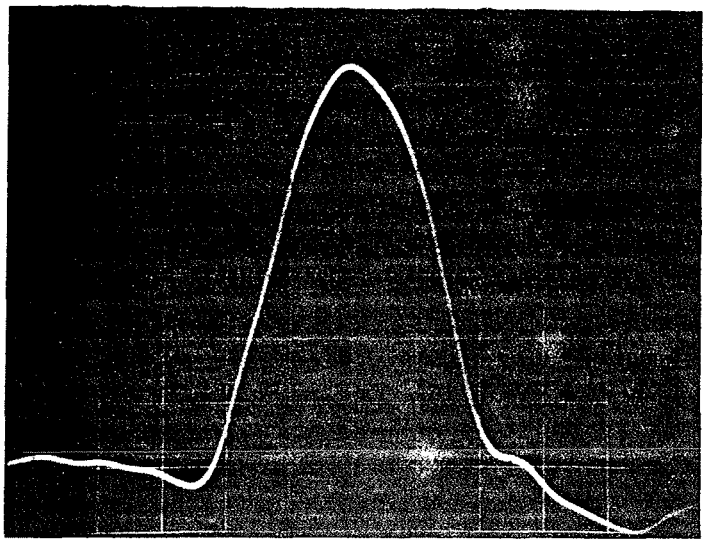

Figure 6. Oscillograph tracing of typical force pulse produced by a hydroacoustic impact tool, recorded with a strain gage mounted on a rotating drill steel.

Oscillator Frequency. Frequency was readily determined from the time intervals between pulses displayed on the oscilloscope.

Amplitude of Pile Vibration. Amplitude was measured with a direct trace. In this method the recording medium was paper which was fastened directly on the pile, and a trace was made on it by rapidly moving a pencil horizontally. Figure 7 illustrates a typical trace.

Static Bearing Capacity. The basic test procedure involved measuring pile settlement using equal load increments. Each increment was about one-tenth of the estimated load needed for progressive settlement of the pile. The time intervals were 2 minutes. A curve of load vs settlement was plotted from which the corner was projected as the bearing load capacity [11].

The interval between driving and bearing load capacity tests was two weeks. The short duration is not considered significant due to the cohesionless soil (beach sand) used in the test. Also, only one cycle was undertaken for the test per pile primarily due to the bearing capacity being the sole data point required.

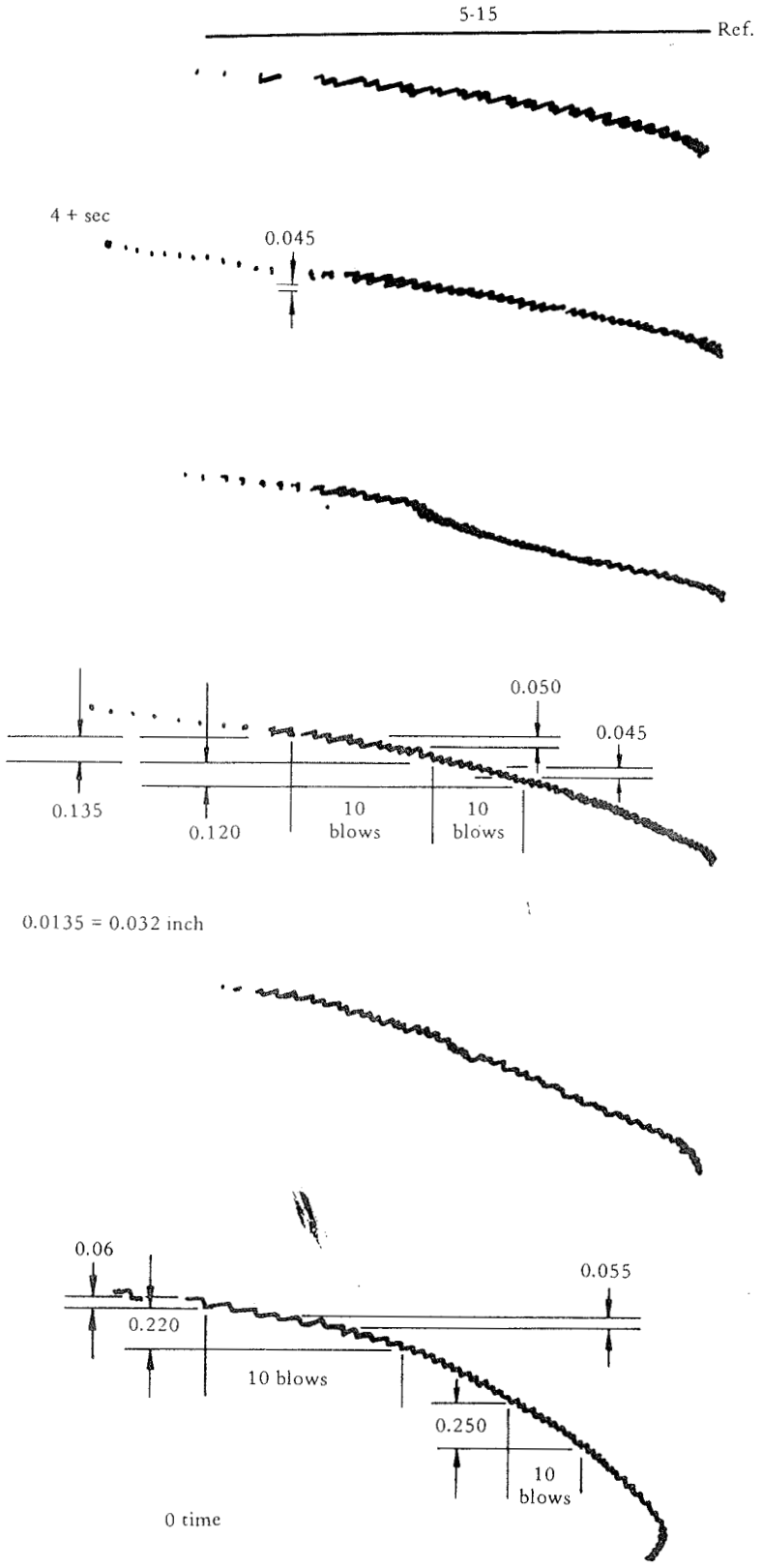

Figure 7. Typical pile vibration trace. Conditions: Site 1; Drive 2; 20-foot pipe; 4-inch OD; closed end.

Test Results

Results achieved from the tests and examination of the hydroacoustic pile driver are limited. Both test sites resembled that of a typical shore area. Clays found to be detrimental to vibratory drivers were not tested. Implications of the test results and conclusions drawn from them are examined more completely in the discussion and conclusion.

Table 1 illustrates the type of data recorded for each pile drive. Figures 8 through 16 consist of typical data recorded for each specific type of driving test and illustrate the energy, penetration velocity and maximum force delivered to the pile as a function of penetration depth. Below the plot graph are the average values of oscillatory frequency, pressure drop across the driver, driver efficiency, flow rate, and surcharge. Driver efficiency is the ratio of the mean energy rate recorded from the pile or adapter divided by the driver input hydraulic power. Figures 17 through 24 are the results of the boring logs at each test site.

The static bearing-load capacity determined by experiment differed appreciably from the value calculated from the Modified Engineering News (MEN) Equation (5). A 20 foot closed-end pipe pile embedded 16 feet vertically at the CEL compound was found by test to have a static bearing-load capacity of 22,000 pounds. The energy transmitted per blow to this pile was recorded as 65 ft-lb per blow with a net pile penetration amplitude of 0.068 inch at 16 feet. If the pile soil resistance were assumed constant and equal to the static bearing load, the pile would absorb 135 ft-lb. This clearly indicates that some form of soil fluidation occurs precluding any application of the MEN formula. Similar results were also found with the other piles tested.

DISCUSSION

The technique of rapidly impacting a pile with a tuned hydroacoustic hammer is presently being proposed as an aid in achieving high pile-penetration rates in soils. The objective of this project is to investigate the increased performance achievable utilizing rapid-impacting pile hammers, to test and evaluate an existing model of a 4-inch rapid-impacting pile driver to determine its potential for further development, and to develop a full-scale prototype if warranted by test results. In this paper a general macroscopic analytical study of the soil-pile relationship is made to compare the major pile-driving theories from which some basic conclusions are drawn.

It has been proven that soil reacts nonlinearly with a rapid pile-penetration rate using high frequency [12, 3]. Many theories have been enumerated based on substantial experimentation over the past decade [2, 3, 6, 12, 13, 14, 15, 16]. For this reason only the highlights of the more generally accepted theories will be discussed here.

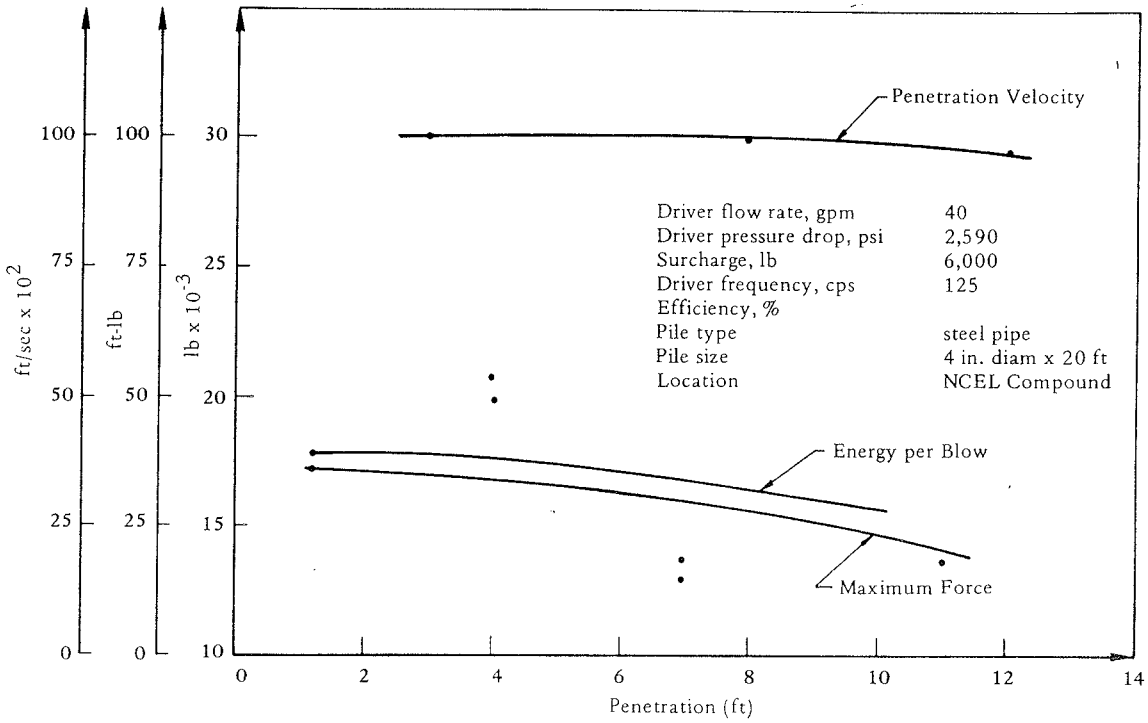

Figure 8. Results of test of 4-inch-diameter by 20-foot steel pipe pile at CEL.

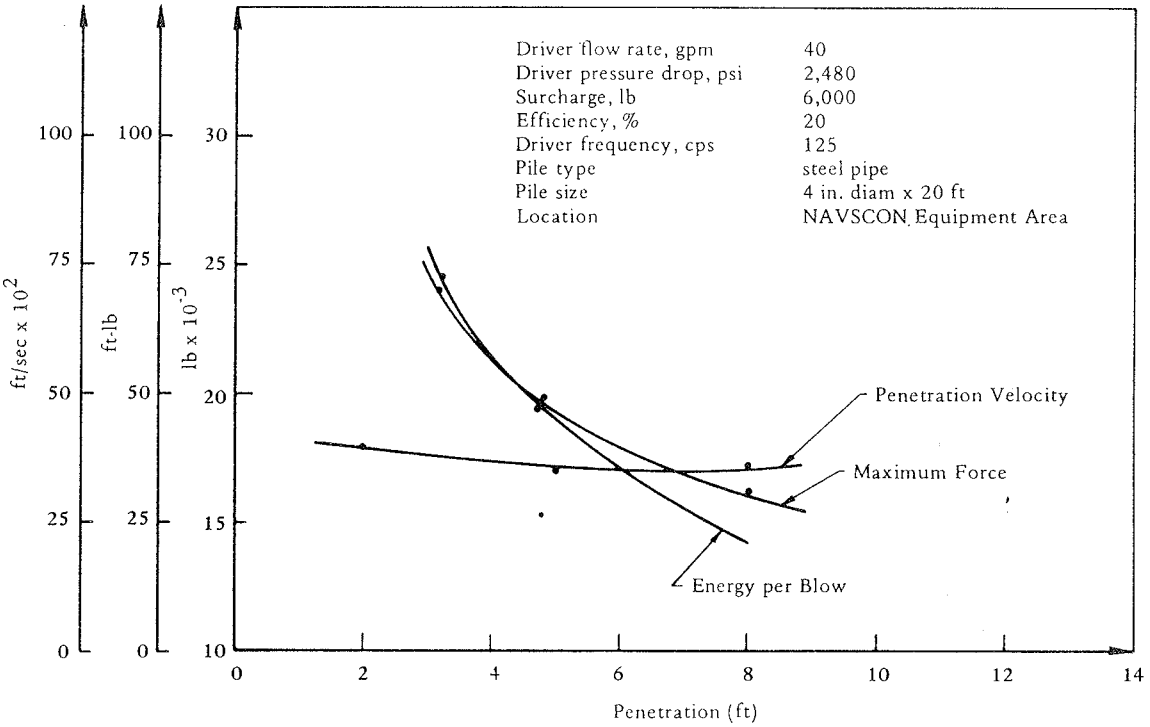

Figure 9. Results of test of 4-inch-diameter by 20-foot steel pipe pile at NAVSCON.

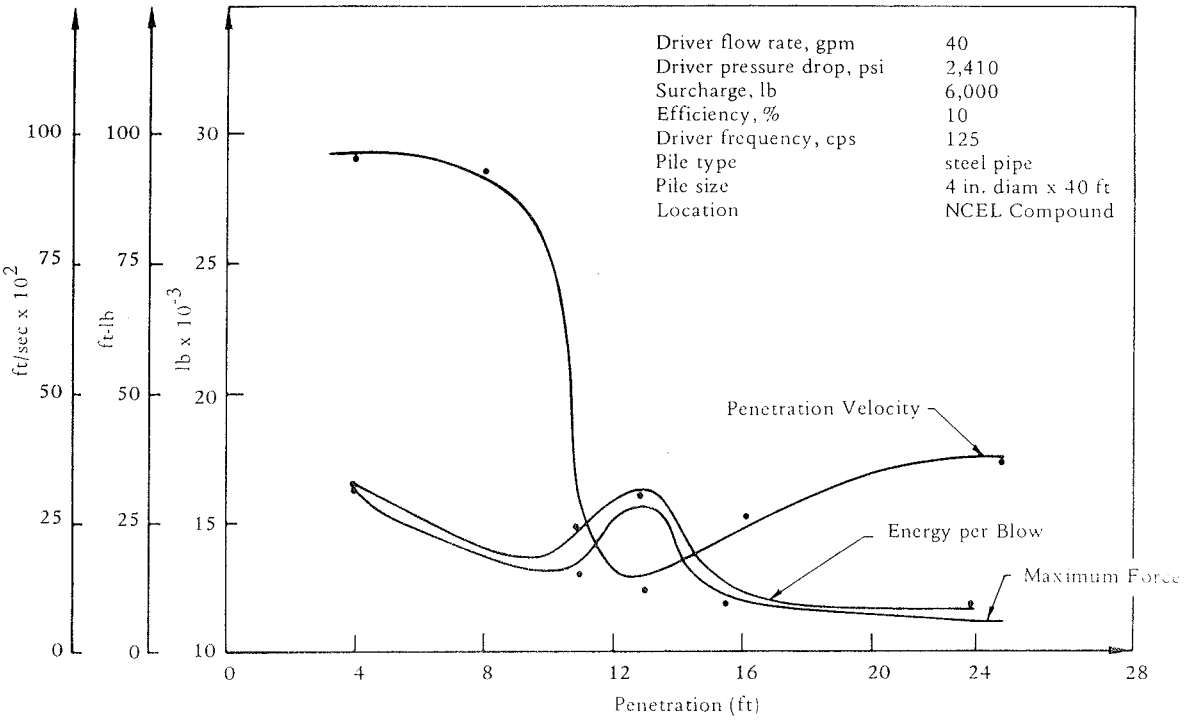

Figure 10. Results of test of 4-inch-diameter by 40-foot steel pipe pile at CEL.

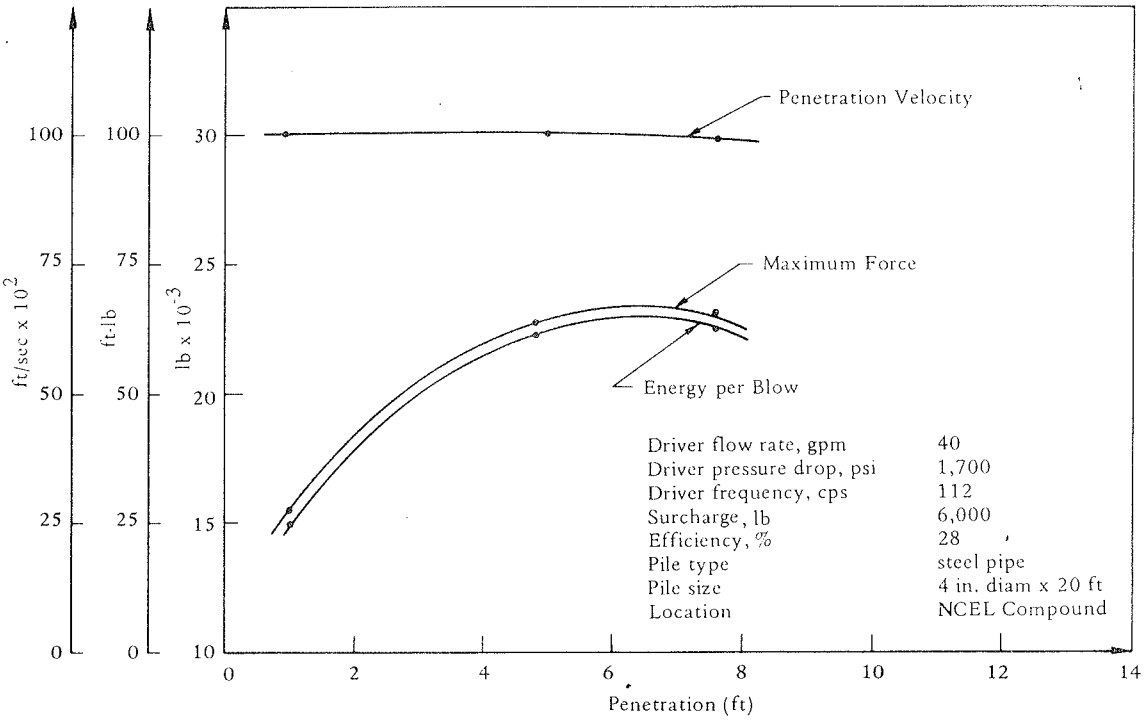

Figure 11. Results of test of 4-inch-diameter by 20-foot steel pipe pile at CEL in horizontal drive and dry conditions.

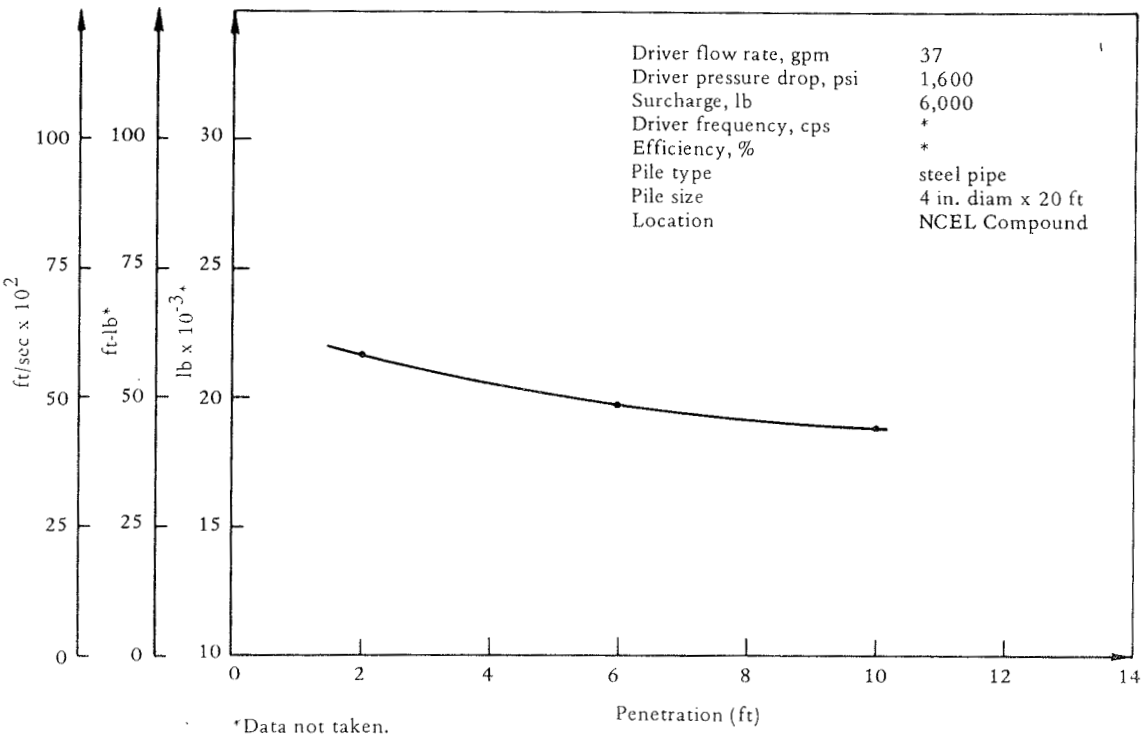

Figure 12. Results of test of 4-inch-diameter by 20-foot steel pipe pile at CEL in horizontal drive and wet conditions.

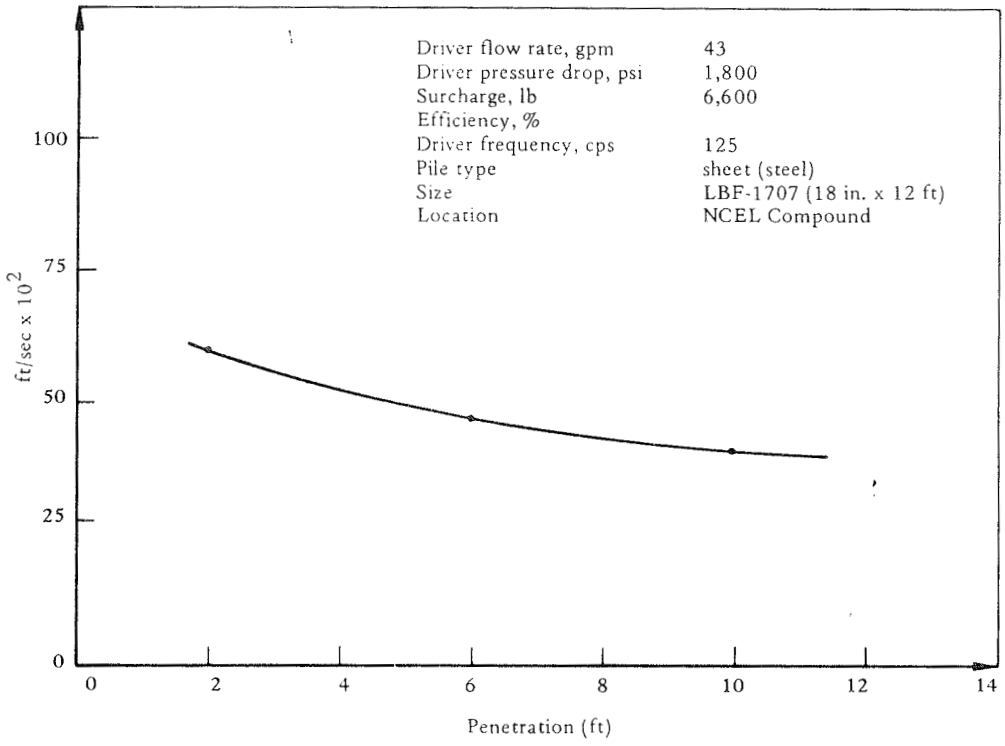

Figure 13. Results of test of sheet steel LBF-1707, 18 inches by 12 feet at CEL.

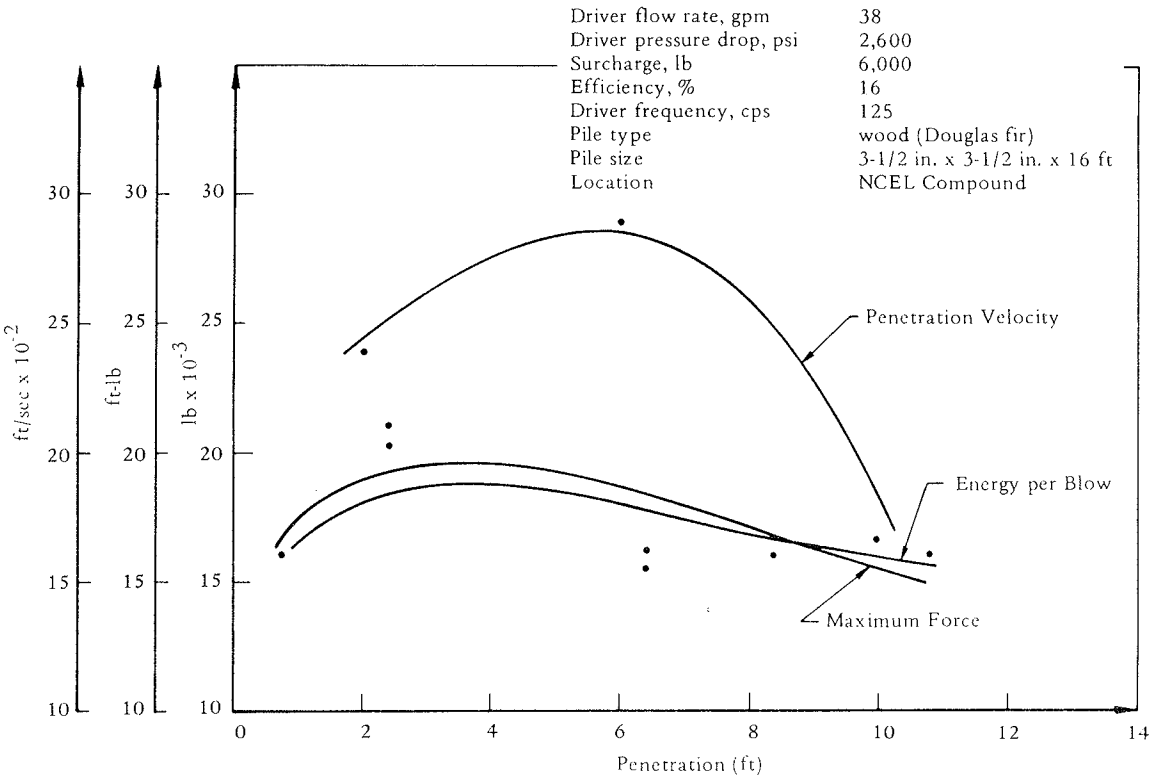

Figure 14. Results of test of Douglas fir wooden pile, 3-1/2 by 3-1/2 inches by 16 feet at CEL.

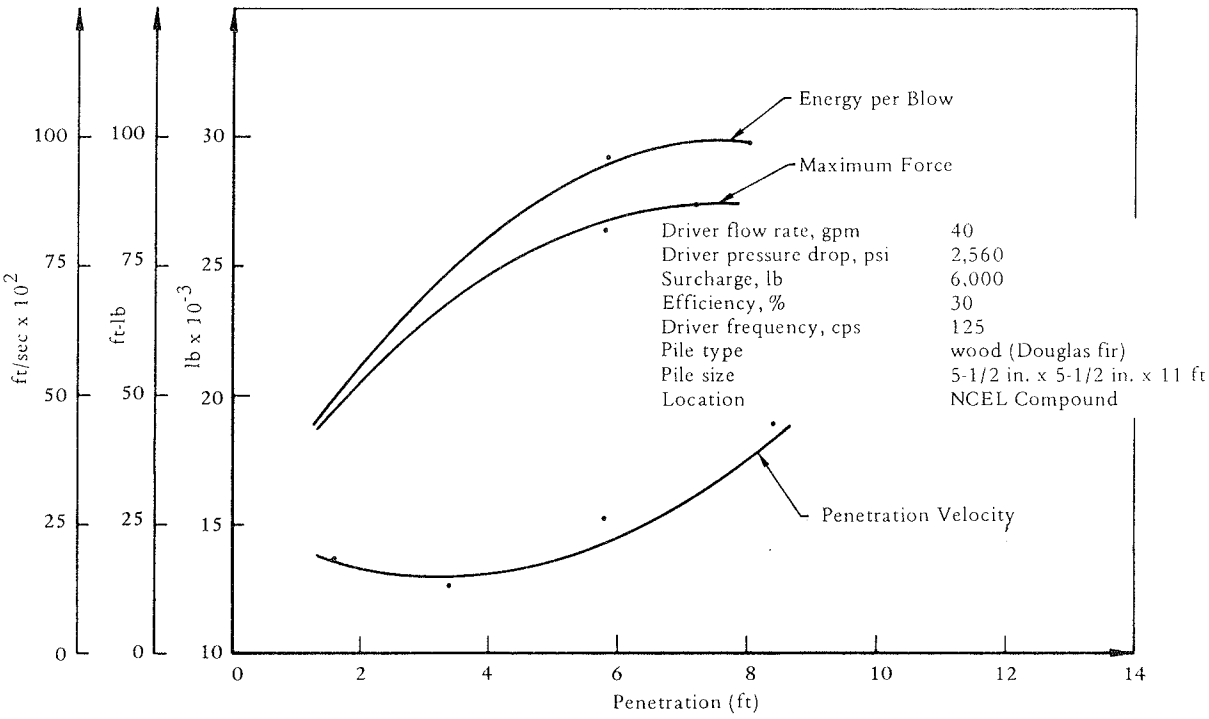

Figure 15. Results of test of Douglas fir wooden pile, 5-1/2 by 5-1/2 inches by 11 feet at CEL.

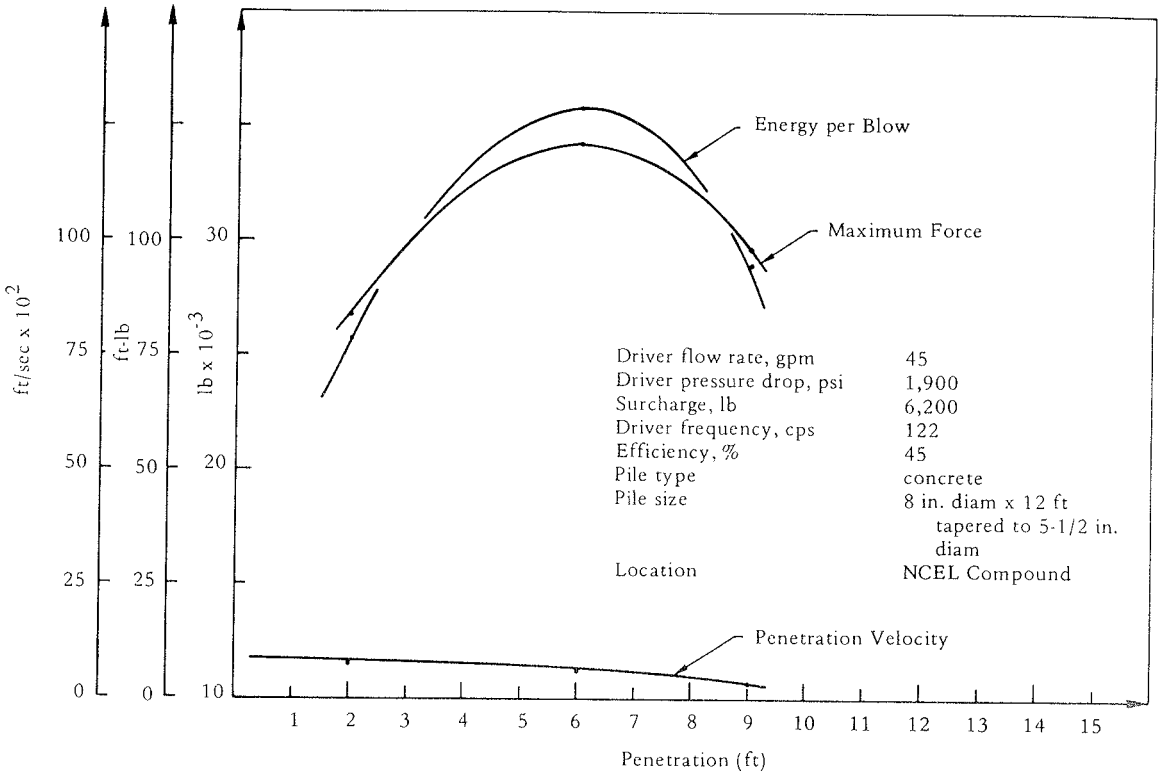

Figure 16. Results of test at CEL of concrete pile, 12 feet long and tapered from 8 inches to 5-1/2 inches in diameter.

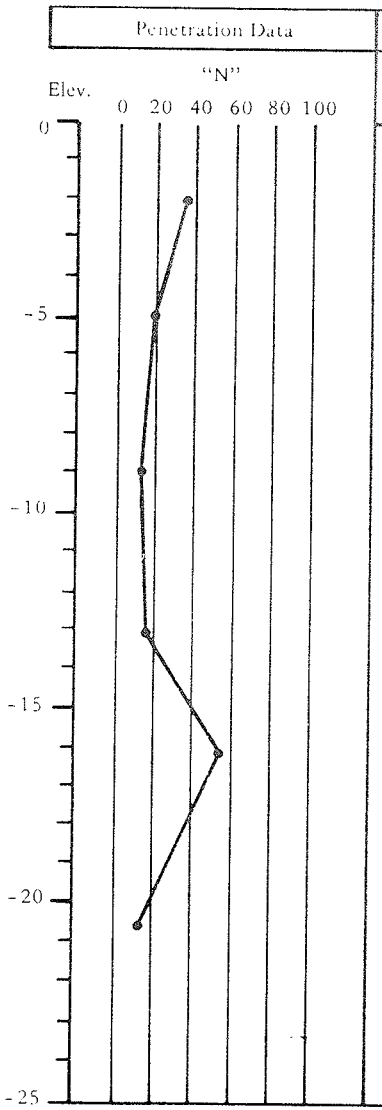

Penetration Data		Boring Log			Soil Properties			
Elev.	"N"	"N"	Note 3	Description	Moisture Content, %	Unified Soil Class.	Liquid Limit	Plasticity Index
0		27	2.0	Dark brown clayey silt				
-5		19	5.0	Becomes light brown at -5 ft, approaches a sandy silt	22.9	ML	35	11
				Water level is -6 ft				
-10		13	9.0	Light grey sandy silt. Some caving of hole from -9 ft to -13 ft.	26.6	ML	26	4
		17	13.0	Grading to a fine to medium sand at -13 ft		SP		
-15		53	16.0	Occasional gravel to 3/4 in.		SP		
-20		15	20.5	Very fine sandy silt	33.2	ML	31	5
				End of boring at -21.5 ft				
-25								

Notes: (1) "N" is number of blows required to drive a 2-in.-OD, 1-3/8-in.ID sampler 1 foot with a 140-pound hammer falling 30 inches.
(2) Elevation is assumed 0.0 foot at ground surface.
(3) Sample depth is at the sampler bottom before driving.

Figure 17. Boring log, NAVSCON equipment area, 11 January 1973.

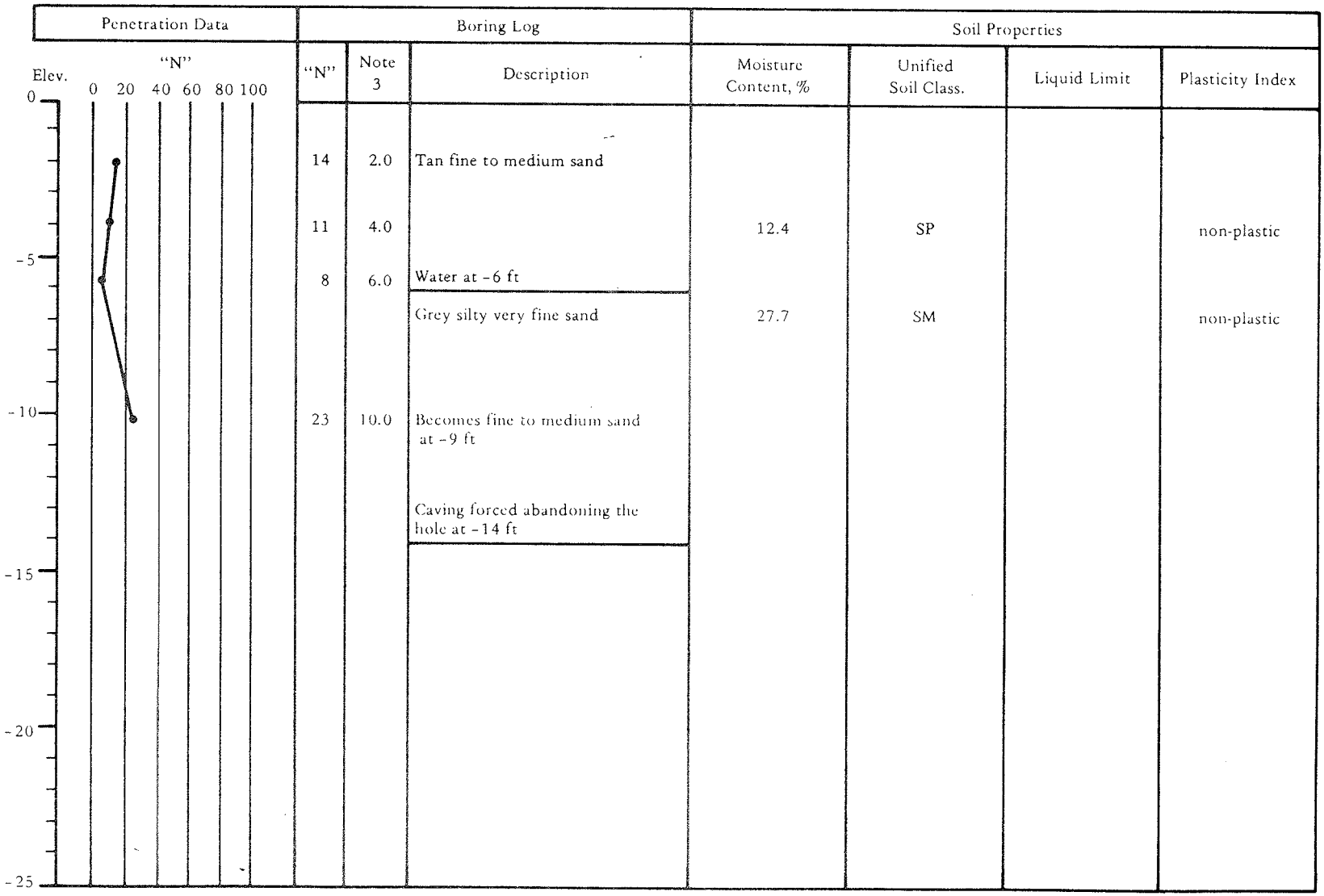

Notes: (1) "N" is number of blows required to drive a 2-in.-OD, 1-3/8-in.-ID sampler 1 foot with a 140-pound hammer falling 30 inches.
(2) Elevation is assumed 0.0 foot at ground surface.
(3) Sample depth is at the sampler bottom before driving.

Figure 18. Boring log, CEL compound behind Building 557, 10 January 1973.

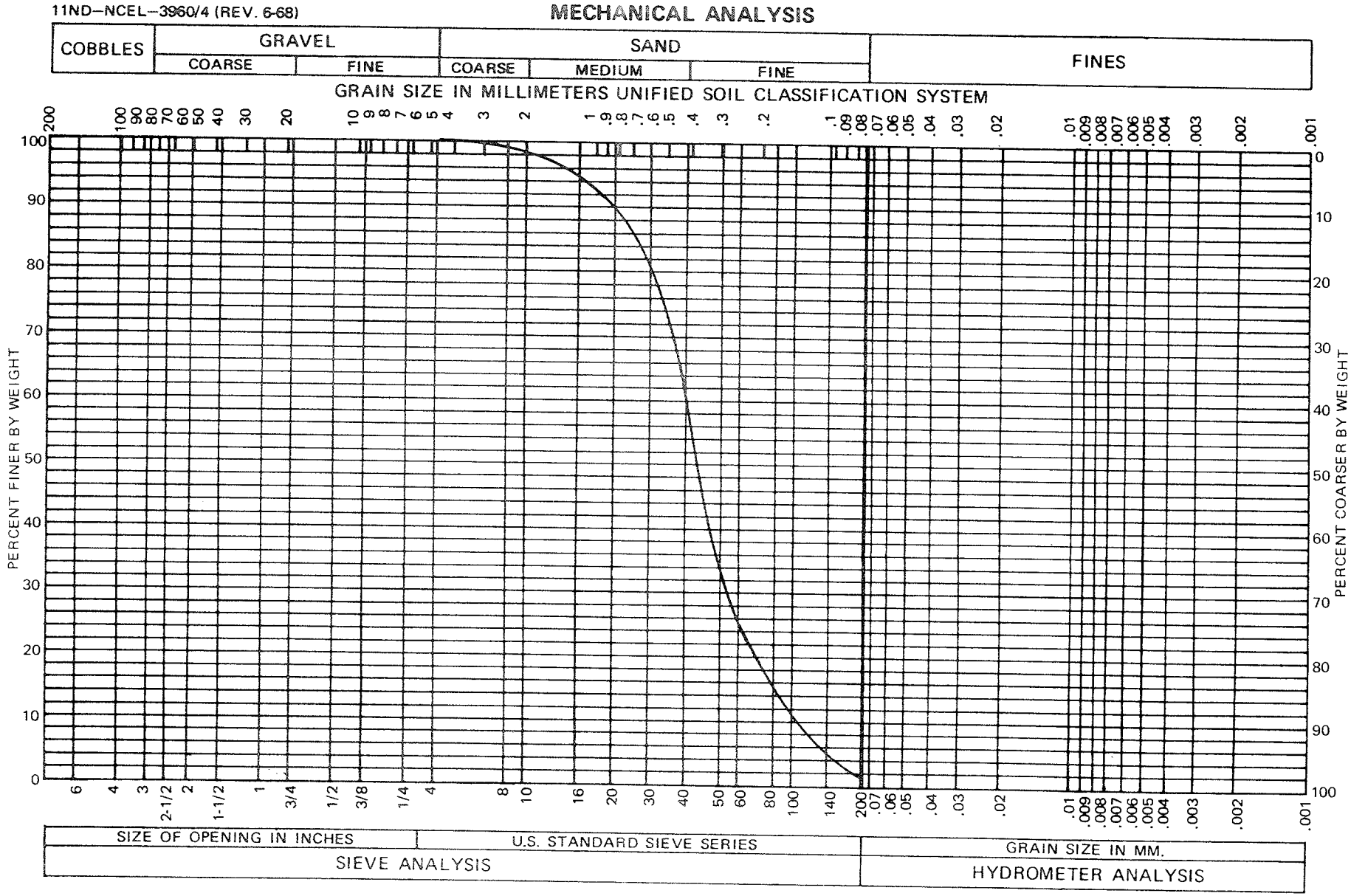

Figure 19. Copy of sieve analysis at CEL, -4 to -5.5 feet.

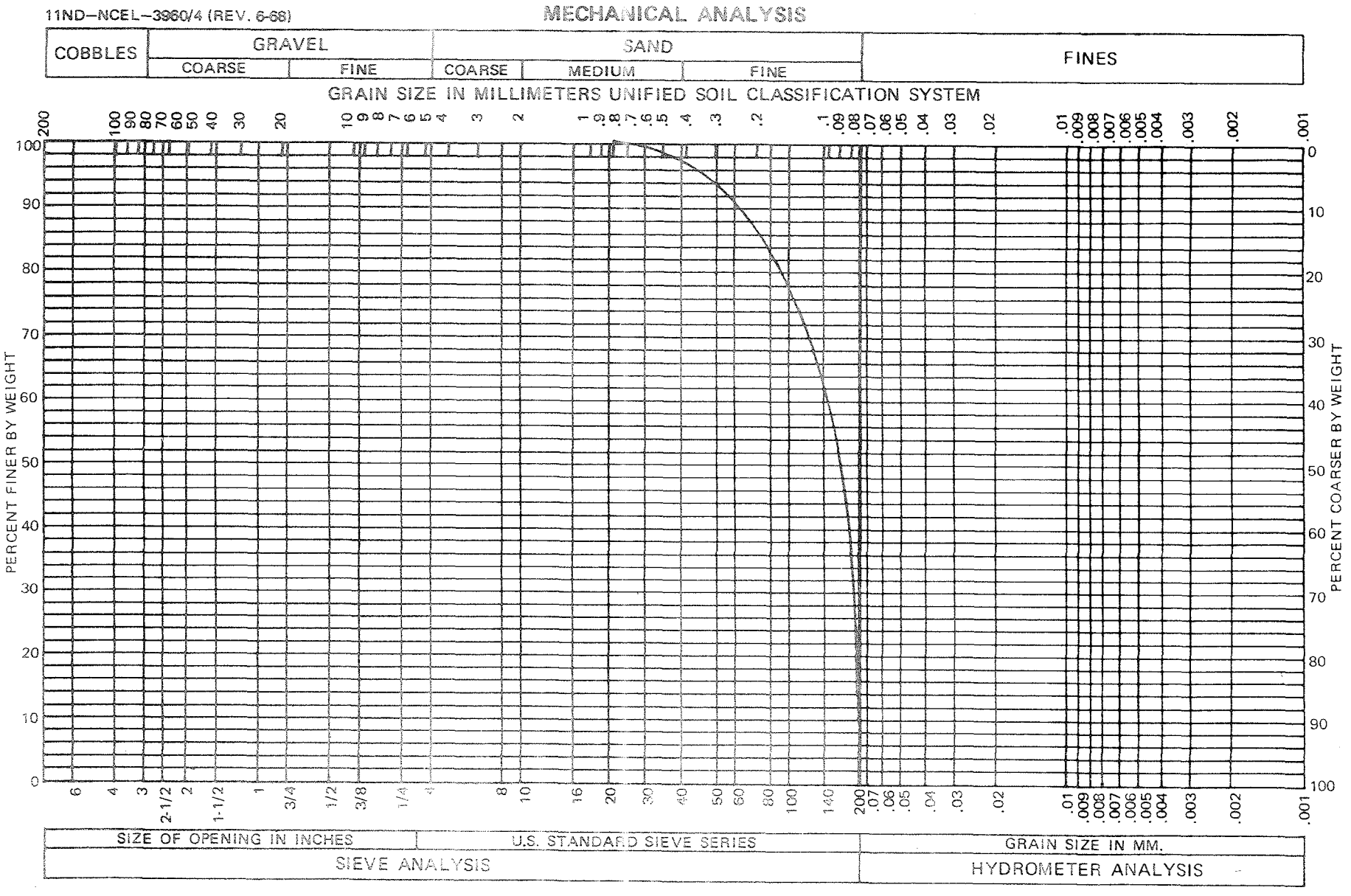

Figure 20. Copy of sieve analysis at CEL, -6.0 to -7.0 feet.

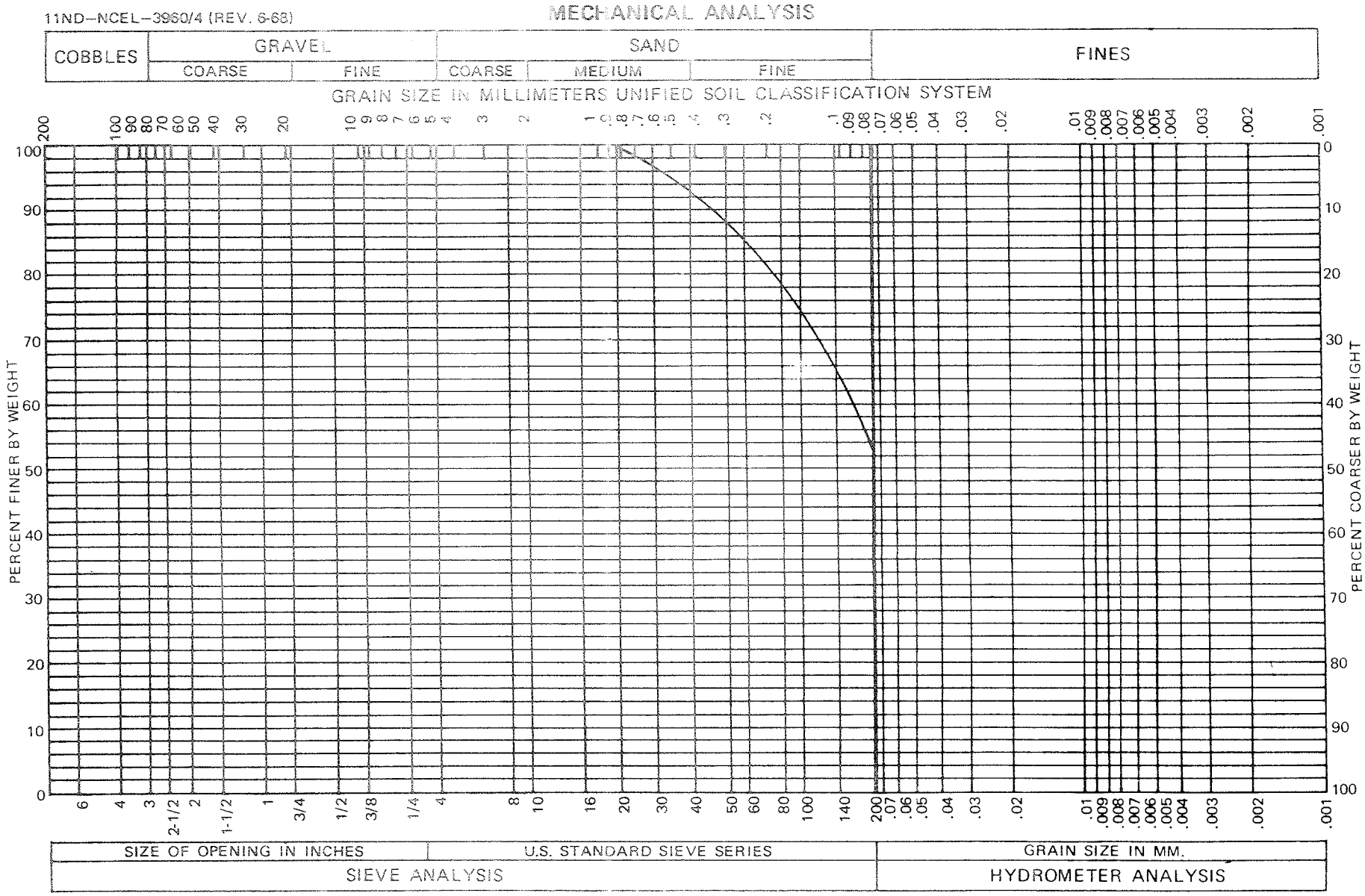

Figure 21. Copy of sieve analysis at NAVSCON area, -5.0 to -7.5 feet.

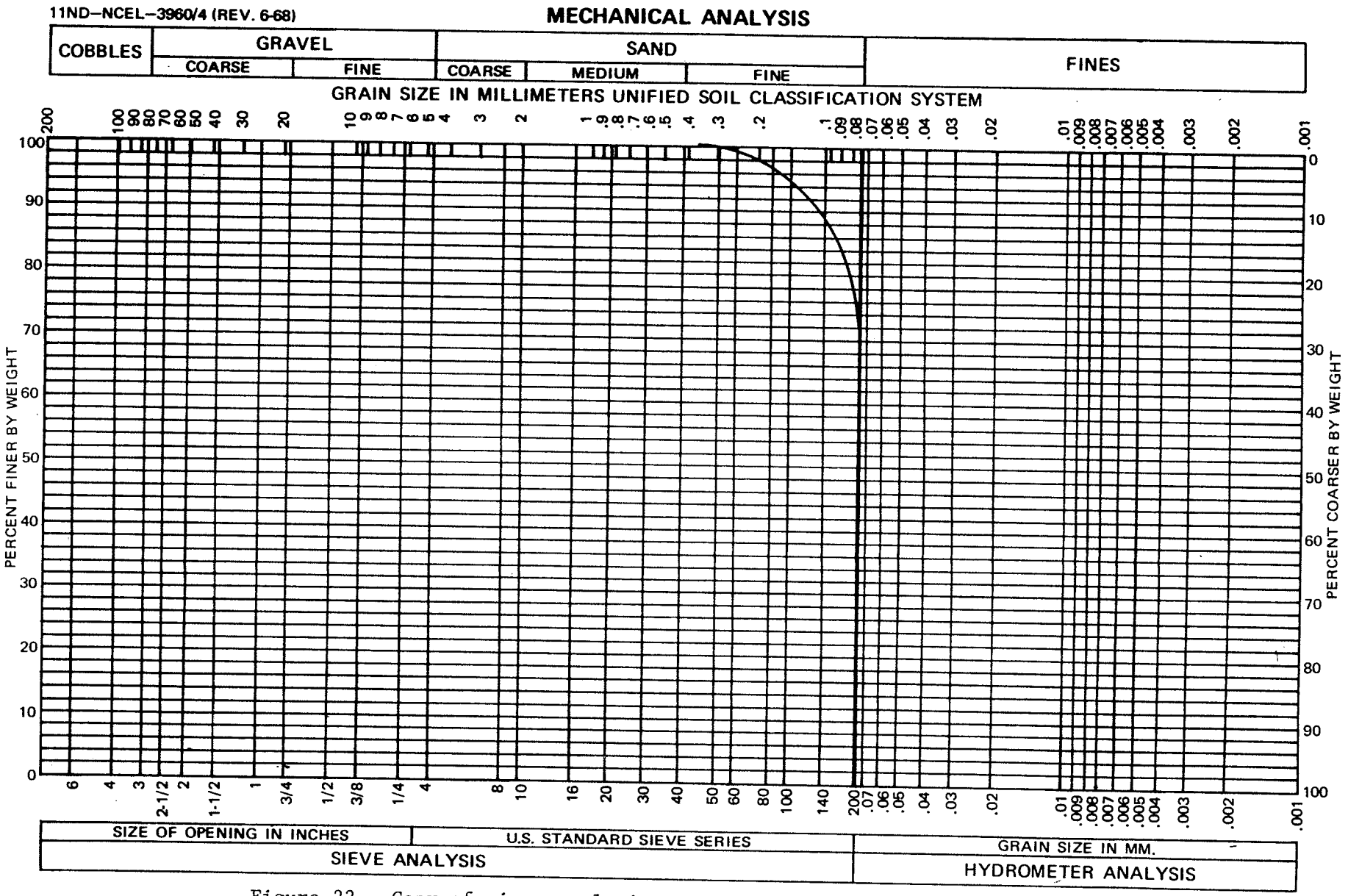

Figure 22. Copy of sieve analysis at NAVSCON area, -9.0 to -10.5 feet.

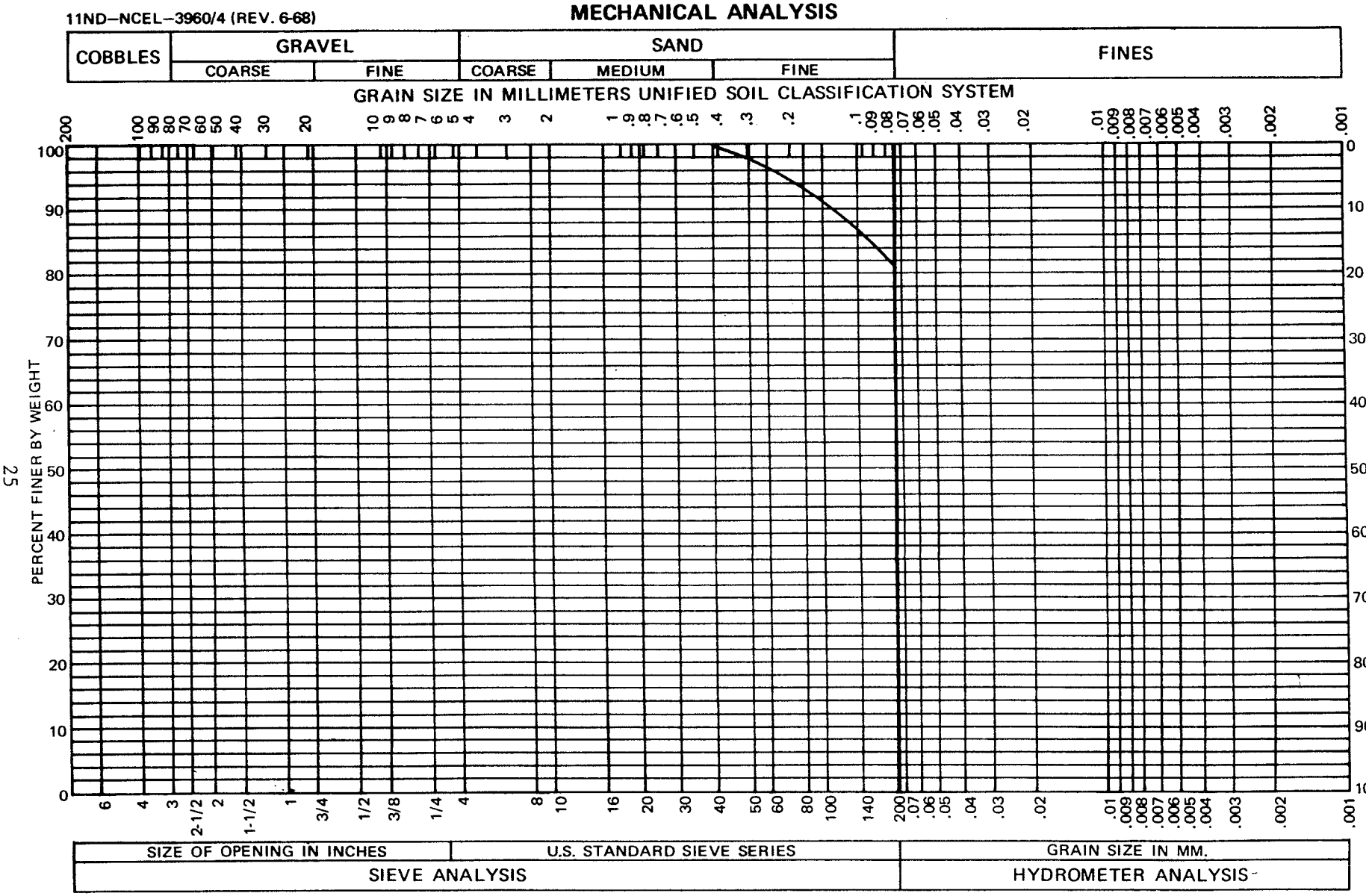

Figure 23. Copy of sieve analysis at NAVSCON area, -20.0 to -21.5 feet.

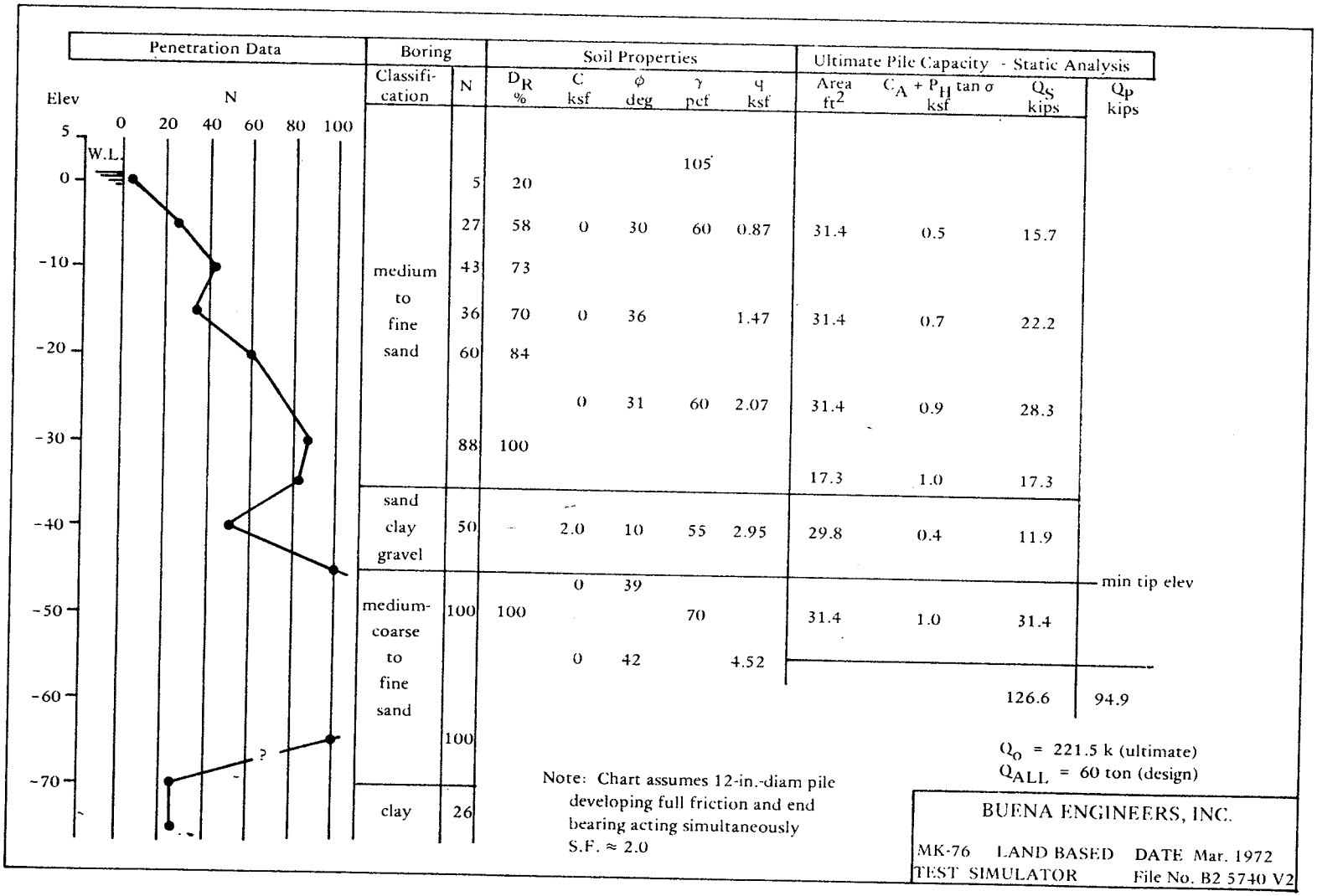

Figure 24. Copy of test of Mk 76 land-based test simulator, March 1972.

In general, considering only high frequency driving above 10 cps (rapid-impacting and vibratory), there are two schools of thought as to what the optimum frequency should be for a particular soil-pile combination. First, in the opinion of many soils experts, the most efficient frequency for rapid pile driving is the frequency tuned to the natural frequency of the soil [12,14,17,18]. The second theory predicts optimum performance at the natural frequency of the pile; i.e., the ''sonic frequency'' [19,20]. The sonic pile driver theory held by Bodine concludes that a tuned pile enhances pile radial vibrations as well as longitudinal because of the Poisson effect [3]. This added variation of the pile radius might cause partial separation of the soil, thereby reducing side friction along the buried portion of pile. The theory is most interesting and could be quite valid; however, in the opinion of some soils experts, the side friction at most absorbs only 10 to 20% of the energy supplied to the pile [12]. In fact, Schmid has considerable experimental data indicating that the side friction is negligible compared to the point resistance. Additionally, Poisson's ratio varies from one pile material to another which could limit the applicability of such a technique. Schmid also proclaims that much of the friction found in soil is viscous rather than coulomb type (independent of velocity) which would be quite detrimental to high frequency driving [12].

It is in the modeling of the soil where most analytical complications are found. The pile may be accurately modeled with the wave equation [8,9] or a finite element technique [3], but when either method is applied to a soil-pile system the solution tends to be inadequate. Soil characteristics vary greatly between coarse sand and clay. Variations of water content in any particular soil sample could change the soil properties considerably [21].

The schematic diagram, Figure 25, is one model of the point resistance; i.e., that resistance found at the penetrating tip of the pile [13]. The variables Q, C_p, and k_p are dependent on the soil and depth beneath the ground surface. Q, ground quake, is defined as that pile-penetration amplitude which the driver must exceed per impact or the soil spring will return the pile to the original position, for a net penetration of zero. The side effects, or resisting forces along the pile, although usually assumed negligible, may be approximated by a combination of coulomb and viscous friction [12,13]. Additional soil ''springs'' would be required for the sonic frequency range because the pile does not behave as a single unit. This problem lends itself to a finite element solution. The ''soil fluidation'' caused by partial separation of the soil and pile due to the enhanced radial vibration has not been modeled to date. If this effect indeed occurs significantly, the side friction could be changed to a dependent variable. It should be pointed out here, however, that there is obviously a trade off between model accuracy and its practical application.

The sonic frequencies range from a low of about 100 cps and upwards for 100-foot steel pile, whereas natural frequencies for soil are between 20 and 25 cps [21]. The ideal solution, if possible, could be

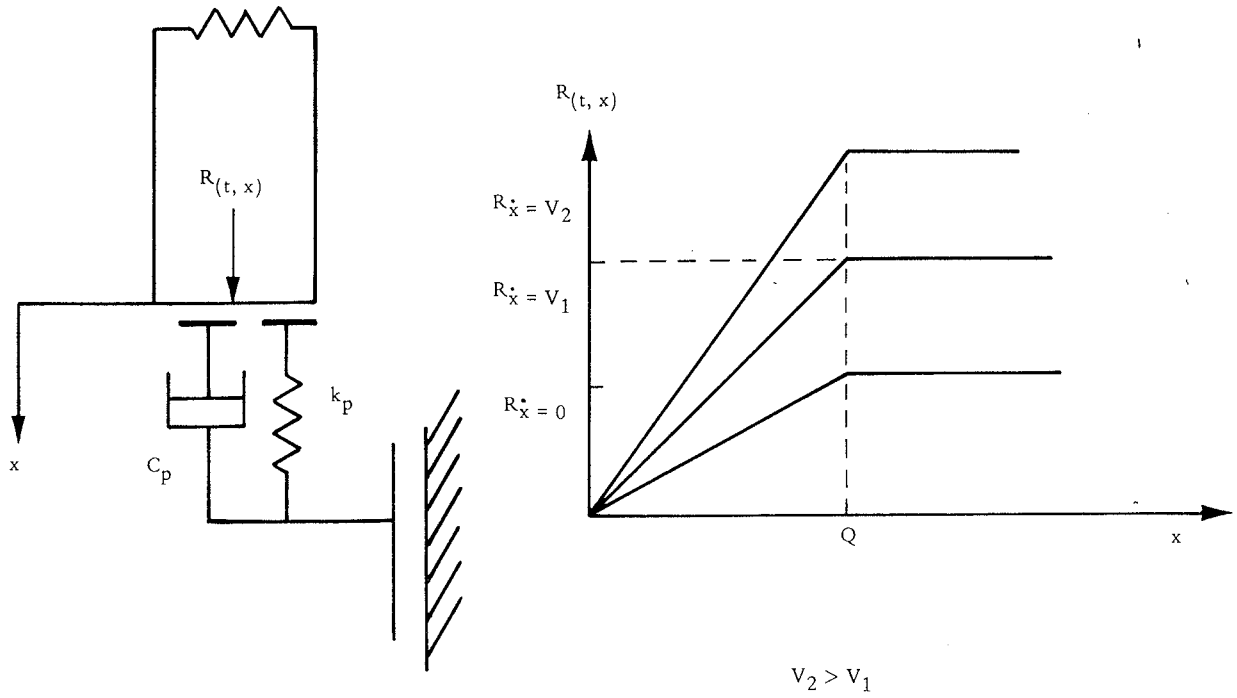

Figure 25. Gharahamani's schematic diagram of nonlinear pile point resistance.

a pile and pile driver with a tuned frequency equal to the sonic and soil frequencies. But the problem with such a solution is three-fold: (1) the soil properties change with depth due to soil variation and pressure; (2) part of the pile side friction is viscous; and (3) the point resistance increases with velocity. A minimum pile amplitude must also be exceeded for ground quake if the model, Figure 25, is correct.

Another possibility for increasing energy efficiency could be a wave shaping of either the forcing function or pile acceleration. For example, if ground quake could be reached with a minimum damping loss and then impacted, possibly a high energy efficiency could be achieved. One way of attaining this would be to have the surcharge equal to the static ground quake force and the variable force acting somewhat like a dither. Such a technique is theoretically used as a measure of efficiency by Bernhard as shown below. In actuality, however, such a high surcharge would buckle most piles.

$$\Pi = \frac{F_p \, V_{av}}{P} \left(\frac{\rho}{L}\right) \tag{9}$$

where Π = efficiency factor

F_p = static bearing load capacity

V_{av} = average penetration velocity

P = driver power input

ρ = length of pile penetration

L = length of pile

The widely varying soil properties and the equally varying theoretical interpretations are not the only confusing clouds covering the horizon of pile-driving phenomena.

Energy and Power Relationships

Energy, in foot-pounds, is the most common unit used for comparing the single-impacting drivers; and power, in foot-pounds per second, is used to compare the high-frequency and rapid-impacting devices. The interesting aspect of both is that neither energy nor power adequately describes the driver capability or driving rate. To best explain why these properties do not give the whole picture, an example will be given.

First, assume that a pile is embedded a known displacement in the ground. Also, assume that the static bearing load is known and is defined as the static force required to further displace the pile in the ground. To simplify, assume that the static and dynamic bearing load capacities are equal and that soil fluidation does not occur. If the impact by the driver occurs over a short period of time (t_o), and the pile plus clinging soil (pile-soil mass equivalent) is large compared to the hammer, then

$$\int_0^{t_o} F(t)\, dt = MV\,(1 + e) \qquad (10)$$

where $F(t)$ = force as a function of time applied to the pile

M = mass of the hammer

V = velocity of hammer just prior to impact

e = coefficient of restitution

Now if $F(t)$ is assumed to be a one-half sine function (first 180 degrees), the integral may be integrated as shown below,

$$\int_0^{t_o} F(t)\, dt \simeq \frac{2t_oF_o}{\pi} \qquad (11)$$

where F_o is the maximum force applied to the pile. From the well-known expression for kinetic energy, $E = (1/2)MV^2$, the velocity as a function of energy and mass may be written:

$$V = \sqrt{\frac{2E}{M}} \tag{12}$$

By combining Equations 10, 11, and 12, F_o may be found:

$$F_o \simeq \frac{\pi(1 + e)}{t_o} \quad \frac{ME}{2} \tag{13}$$

As a result, F_o is found to be a function of the impacting mass, impact duration, input energy, and coefficient of restitution. One may deduce that if F_o is less than the bearing load, further penetration is not possible. In fact, if the energy is doubled and the time duration is increased by two, without changing the mass, no change in F_o would occur. Also, if the impacting rate (number of blows per second) were increased it would not alter the answer since this parameter does not appear in the formula. In conclusion, one may deduce that even though the above example is not totally accurate due to the assumptions made, the important revelation that F_o is not a direct function of power or energy is not altered.

One may ask then: if neither power nor energy can be used as a direct indication of driver capability, what should be used? The answer is not elementary, but if one has to make a valid comparison with limited analytical data, the best comparison would have to be the force, F(t), applied to the pile and its time duration, t_o. Obviously, if a force larger than the bearing load is applied to the pile for a sufficiently long period, penetration should occur.

Below is a simplifed derivation of the minimum value of force and time duration. A, Q, M, $\bar{F}_p$ and $\bar{F}_o$ are pile acceleration, ground quake, mass of impacted body (pile, anvil, and clinging soil), mean dynamic pile soil resistance and mean applied force from the pile driver, respectively.

$$Q = \int_o^{t_o} \int_o^{t_o} A \, dt \, dt$$

$$\simeq \int_o^{t_o} \int_o^{t_o} \frac{\bar{F}_o - \bar{F}_p}{M} \, dt \, dt$$

$$Q \simeq \frac{\bar{F}_o - \bar{F}_p}{2M} t_o^2 \qquad (14)$$

Therefore, the boundaries for F_o are

$$F_c > F_o > \frac{\pi}{2}\left(\frac{2MQ}{t_o^2}\right) + F_p \qquad (15)$$

where F_c is the pile yield force or force required to buckle the pile in t_o seconds. If the forces are approximated by a clipped sine function, then it can be assumed that the maximum forces F_o and F_p are equal to $\pi/2$ times the mean force, respectively. For a rough estimate the peak force F_o is about 1.5 to 3 times the static bearing capacity F_p, and t_o is usually small enough to allow F_c to be equal to the pile yield force for present single impact hammers. Results of the hydroacoustic hammer on the 20-foot pile embedded 16 feet, cited above, produced a maximum force of 31,000 pounds F_o for a static bearing-load capacity F_p of 22,000 pounds. From the formula of Equation 15 one can determine without extensive testing a rough estimate of the capacity (in pounds) of a pile driver. The formula is conservative and does not include soil fluidation.

Dynamic Pile Formula

The static bearing load capacity of the pile after it has been driven must be estimated by soil testing [5,21], dynamic pile formulas [22] or pile static bearing-load tests [23]. The dynamic pile formula is the least time consuming and will be discussed next.

Figure 26 is a schematic of a single impact driver with W_r equivalent to the ram weight and k is the equivalent spring constant of the drive cap and pile stub (length of pile sticking out of the ground). The product of W_r and h is the maximum energy per blow assuming that the past blow deflection and displacements are small compared to h. If it is assumed that (a) maximum force occurs with maximum deflection of the spring, (b) simultaneously, the maximum force occurs when the pile has been moved one-half of S (net displacement per blow), and (c) half the input energy of the blow at S/2 has been consumed by storage of energy in the ''spring'' (pipe cap) and in work of penetration to distance S/2. The remaining 1/2 of the energy goes to work of penetration to distance S. The following formulas evolve from this:

$$\frac{12hW_r}{2} = \frac{1}{2} k\bar{x}^2 + \frac{S}{2} F_p \qquad (16)$$

where $\bar{x}$ is the maximum spring compression and h is multiplied by 12 to convert all terms to lb-in. The above equation would be representative of impact if there were no impact losses or rebound; however, this is not the case. Energy losses must be considered; a commonly used equation for impact is:

$$E_2 = \frac{\frac{1}{2}(1 - e^2)(M_r M) V^2}{M_r + M} \tag{17}$$

where M_r = impacting mass

M = impacted mass

V = velocity of impacting mass

e = coefficient of restitution

It is assumed that the impacted mass velocity before and after impact and the associated kinetic energies are negligible. Equation 17 is subtracted from the input energy $12hW_r$ of Equation 16 and if masses M and M_r are converted to weights W and W_r by g, gravity, the following equation would evolve:

$$\frac{12W_r h}{2}\left(\frac{W_r + We^2}{W_r + W}\right) = \frac{1}{2} k\bar{x}^2 + \frac{S}{2} F_p \tag{18}$$

Note that W, the impacted weight, in most cases should include a portion of the pile driver weight. Figure 27 (also found in Reference 5, page 135) is a plot of calculated energy transmitted to the pile versus energy measured. In this figure an inaccuracy exists because W consists only of the pile and anvil. More accurate results, marked with a +, include the weight of the driver. W for the hydroacoustic driver would consist of the pile weight and anvil only and would not include the weight of the driver housing because there is no damper interconnection between the anvil and the housing of the hydroacoustic driver [4,7,24,25]. As a result, the energy loss during impact is slightly less for the hydroacoustic driver for the same coefficient of restitution.

If Equation 18 is divided by F_p and if the value 0.1 is substituted for $k\bar{x}^2/F_p$ and a ''factor of safety'' of 6 is used on F_p, the following equation, Modified Engineering News (MEN) formula [5], results:

$$F_p = \frac{2W_r h}{0.1 + S}\left(\frac{W_r + We^2}{W_r + W}\right) \tag{19}$$

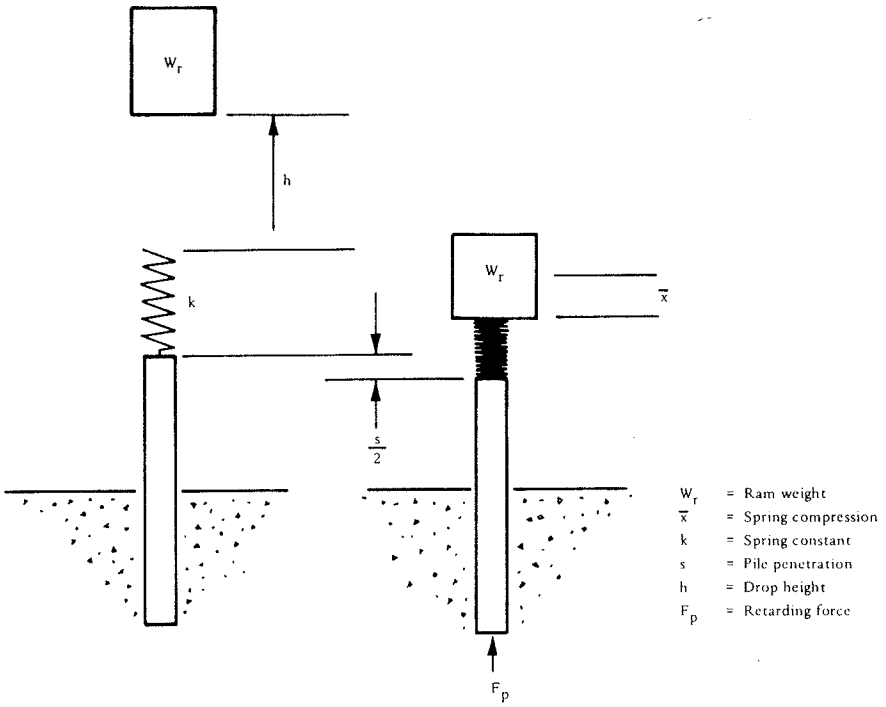

Figure 26. Equivalent model of single-impact driver.

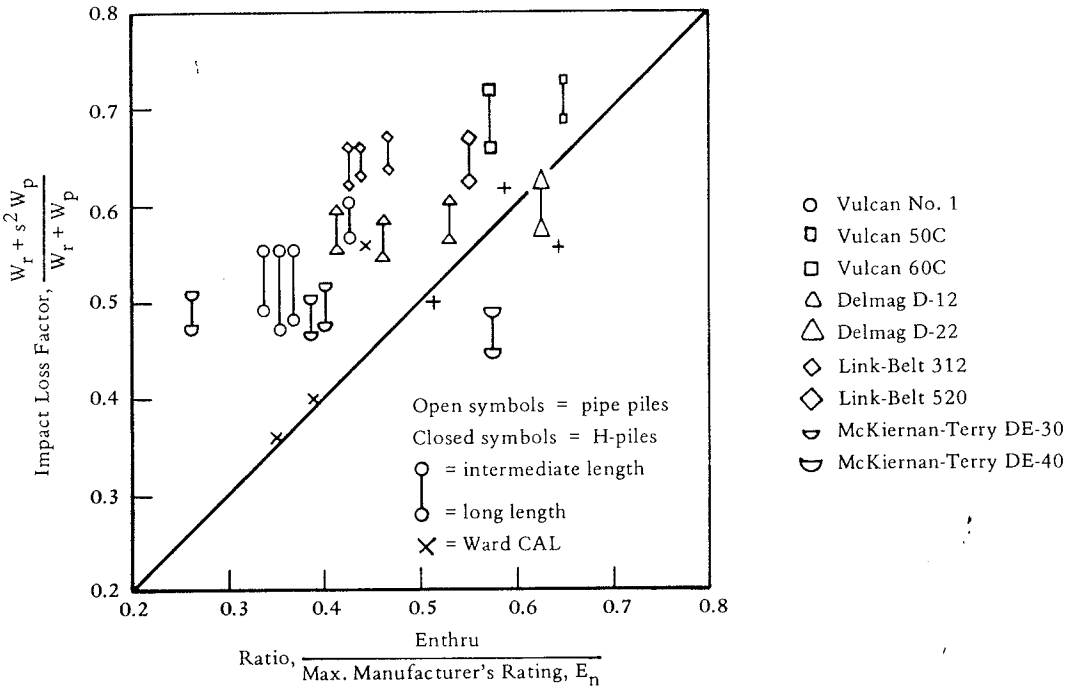

Figure 27. Comparison of impact loss factors from Michigan highway study [5].

The value of 0.1 was empirically derived from field-test data due to k and $\bar{x}$ being difficult to measure on site. The MEN formula is not the only dynamic formula [5,22], but it is one of the simpler equations to work with and appears to have some relevance to the theoretical dynamics involved.

To adapt the MEN formula to the hydroacoustic pile driver, the 0.1 constant and coefficient of restitution should be modified from accumulation of field data for each soil or driving condition in order to predict the static bearing-load capacity. The uncertainty in the dynamic pile formula could not be determined from the CEL test results because of the apparent fluidation of the soil. The static bearing-load capacity F_p is significantly greater than the dynamic shear and frictional soil resistance when fluidation occurs which nullifies the assumption made in the derivation that the work consumed per blow for pile penetration is equal to SF_p.

Vibratory Pile Drivers

The vibratory pile driver does not use impact as do the single-impacting hammers or hydroacoustic driver, but applies a sinusoidal force on the top of the pile in combination with a surcharge. Note in Figure 28 that the two eccentrics are phased so that the force generated is zero in all directions except in the vertical. The force F(t) applied to the pile is given below [26]:

$$F(t) = W_s + (W_d r) \frac{\omega^2}{g} \sin \omega t \qquad (20)$$

where W_s = surcharge

$W_d r$ = eccentric moment

ω = rotating velocity

t = time

For the tandem model 2-60, 240-horsepower motor, the maximum force applied to the pile would be:

$$F_o = \frac{62,000}{2,000} + \frac{6,940}{2,000 \times 32} \left(\frac{900}{60} 2\pi \right)^2 (1.0)$$

$$= 104 \text{ tons}$$

and

$$t_o = 0.033 \text{ sec}$$

where t_o is the time required for the rotating weights to make half a revolution. The equivalent energy per cycle applied to the pile may readily be derived assuming that the applied energy is derived from the momentum exchange of the suspended weight of the driver (Figure 28); i.e.

$$\int_0^{t_o} F(t)\, dt = MV \qquad (21)$$

M and V are mass of suspended weight and velocity. From Equations 11, 12, and 21,

$$E = \frac{1}{2} MV^2 = \frac{2}{M}\left(\frac{F_o t_o}{\pi}\right)^2$$

$$= \frac{2(32.2)}{38{,}000}\left(\frac{104 \times 2{,}000 \times 0.033}{\pi}\right)^2$$

$$= 8{,}000 \text{ ft-lb}$$

Considering the power available, the low energy output and force F_o are not impressive. However, soil resistance might decrease with high frequency vibration; or high impact forces could occur at the pile penetrating tip rather than the pile top. One characteristic of vibratory drivers is that the entire pile must oscillate longitudinally, breaking contact with the soil at the tip and reimpacting which, along with the Poisson effect, works to significantly reduce pile resistance. Of course one may ask, ''If the resistance does decrease, regardless of the cause, how much is the reduction?'' What analytical formula, or what experiment can be used in the field to determine vibratory pile resistance? Many theories and test results are available as stated above, but at present there is not enough available information to predict resistance successfully in a virgin soil with vibratory drivers. Static bearing load of an installed pile with a vibratory driver is not predictable. No empirical or theoretical dynamic pile formula capable of predicting the static bearing-load capacity of a pile driver with a vibrating driver was found by CEL.

Other Driving Techniques

Not included in this study is the Mark I hydraulic pile driver invented and designed by Moog of New York and developed by Raymond International [14]. The Mark I uses a three-stage hydraulic servo

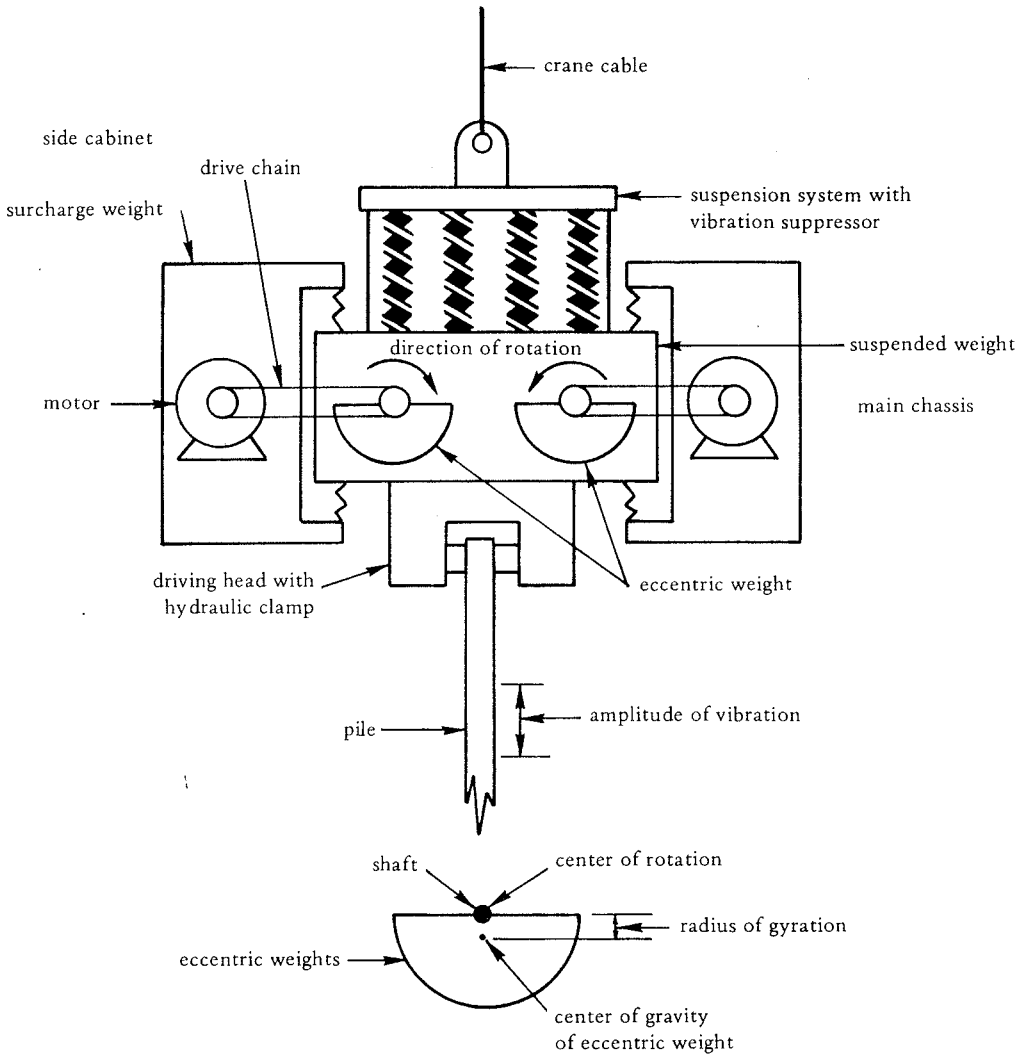

Figure 28. Schematic of eccentric weight vibratory driver.

valve with a pressure drop and flow rate capable of up to 5,000 psi at 150 gpm. The device is still in the testing stage, and the design and test results are held confidential. One may assume, however, that if a servo valve is used, frequency, force wave shape, amplitude, surcharge and suspended weight could be designed as variables and subject to being easily optimized. The drawbacks are susceptibility to failures from oil contamination in the servo and the requirement for sophisticated electrical hardware and operator experience. The results should be made public soon and much should be learned there from.

Another interesting pile driving method could be to drive the pile in with a single impact. An analogy to such a technique is a bow and arrow. A strong bow can easily drive a wooden arrow through a linear yard of sand. In another example, straw has been observed embedded several inches into hardwood trees after a tornado. The principle is simply that of energy transfer; i.e., kinetic energy of the pile utilized for work in penetration. The problems with such a method would be immense due to high viscous friction, safety risks, and trying to estimate pile-penetration depth and bearing capacity.

CONCLUSIONS

To make a clear-cut breakdown of all the known pile drivers and make a single selection of an ideal driver most applicable for Navy utilization is not simple. There exists a large number of techniques available to drive piles. The approach taken in this paper was to group all the various techniques into three basic categories: vibratory (sonic and non-sonic), rapid-impacting, and single-impacting. Obviously there is an arbitrary distinction between rapid- and single-impacting. Rapid-impacting is assumed here to have an impacting rate above 20 cps, a range which includes the natural frequencies of soil.

Of all the known drivers only the diesel and Bodine's engine-mounted sonic vibratory driver are self-contained. The remaining pile drivers require a power supply; i.e., electric, steam, pneumatic, or hydraulic. The Bodine driver essentially has its power supply mounted on the driver and weighs considerably more than a diesel. Making a comparison using a dimensionless ratio of the maximum pile-driving bearing-load capability F_p to the weight of driver plus auxiliary equipment, the diesel would fare well; however, shipping weight is only one factor.

Another factor is the driving rate, or more practically, the total time to drive the pile, which includes set-up time. The problem with comparing driving rates is that they are closely dependent upon the soil composition, most noticeably with vibratory drivers. Soil fluidation can greatly enhance penetration rate. Unfortunately, it is difficult to predict. In fact, viscous forces sometimes attenuate penetration of high-vibratory-frequency drivers but do not affect single-impacting drivers. The rapid-impacting hydroacoustic hammer has not experienced

viscous effects strong enough to stop penetration, but tests with the driver are few. Results from this test program were impressive, nevertheless, with the hydroacoustic driver averaging 30 ft/min penetration rate for wood and steel, and 12 ft/min for concrete. Diesel driving in similar soil by CEL averaged 2.5 ft/min for wood and 1.6 ft/min for concrete [4]. During CEL tests, set-up time took as long as driving time.

The rapid-impacting hydroacoustic pile driver produced a high force on the pile which was rudimentarily derived in Equation 15 in the discussion as the primary parameter for predicting capacity. Also, no special adapter is required on the pile with the impact drivers, single or rapid. The pile static bearing load is roughly predictable with single-impact drivers using dynamic pile formulas. The hydroacoustic driver is a tuned single-frequency driver, and experimentation by altering frequency and impact amplitude is not possible without significantly changing driver hardware. This does not necessarily detract from the device, because one principle advantage is its simplicity of having only one moving part.

The final comparison factor and probably most important is cost effectiveness. This is, as one may expect, the most difficult to calculate. The hydroacoustic driver tested is an experimental model and not an operational full-scale driver. Many problems that may be encountered in the field are unknown. Consequently, a detailed analysis [26] is not given here. If it is assumed that maintenance, down time, and required number of operators are roughly the same for hydroacoustic and diesel hammers, a general comparison can be made. Actually, this assumption is reasonably accurate due to the similar mechanical complexity of each and the manner in which the drivers are used. The set-up time is also about the same, between 10 and 20 minutes per pile. The hydroacoustic driver, averaging 25 to 30 ft/min, could decrease total time per pile by 50% for penetration depths of 25 feet. With three operating personnel, two riggers and one crane operator, the cost saving per pile (at $10 per man-hour) would be between $10 and $15. Cost savings would rise even more with increased penetration depths.

It appears to this observer that considerable information is still needed before a complete analysis can be made to select a single optimum pile driver. However, from all the literature and experimentation to date, the rapid-impacting technique of driving piles appears most promising.

RECOMMENDATIONS

It is highly recommended that the Navy finance a continued investigation of new pile-driving approaches to stay abreast with the latest developments. It is also recommended that an in-house research program be financed to determine which pile-driving parameters are important and how to verify a pile-driver capacity without extensive field tests. The

program need not be expensive and should rely heavily on test data resulting with empirical formulas capable of determining the following specific information:

1. Relationship between pile cross-sectional area, driving rate and ground quake.
2. Dynamic pile formula validity with respect to vibratory and rapid-impacting drivers.
3. Effects of soil fluidation on rapid-impacting hammer.
4. Longitudinal power flow attenuation as a function of penetration depth.
5. Rapid-impacting pile velocity versus dynamic soil resistance.

It is urged that the program produce techniques or test procedures to adequately determine the minimum capabilities of a pile driver. A detailed analytical study should be left for academic institutions.

It will not be necessary to expend Navy funds to finance development of a full-scale prototype hydroacoustic driver since this will be done by Raymond International. Raymond is also doing extensive research with the Mark I high-frequency servo driver. A combination of these two R&D projects plus continual improvements of the diesel should adequately produce or finalize proper selection of the best driver or group of pile drivers suitable for Navy needs. This, however, does not mean that the Navy should discontinue research in this important area.

Appendix

PHOTOGRAPHS OF PILE DRIVING TESTS

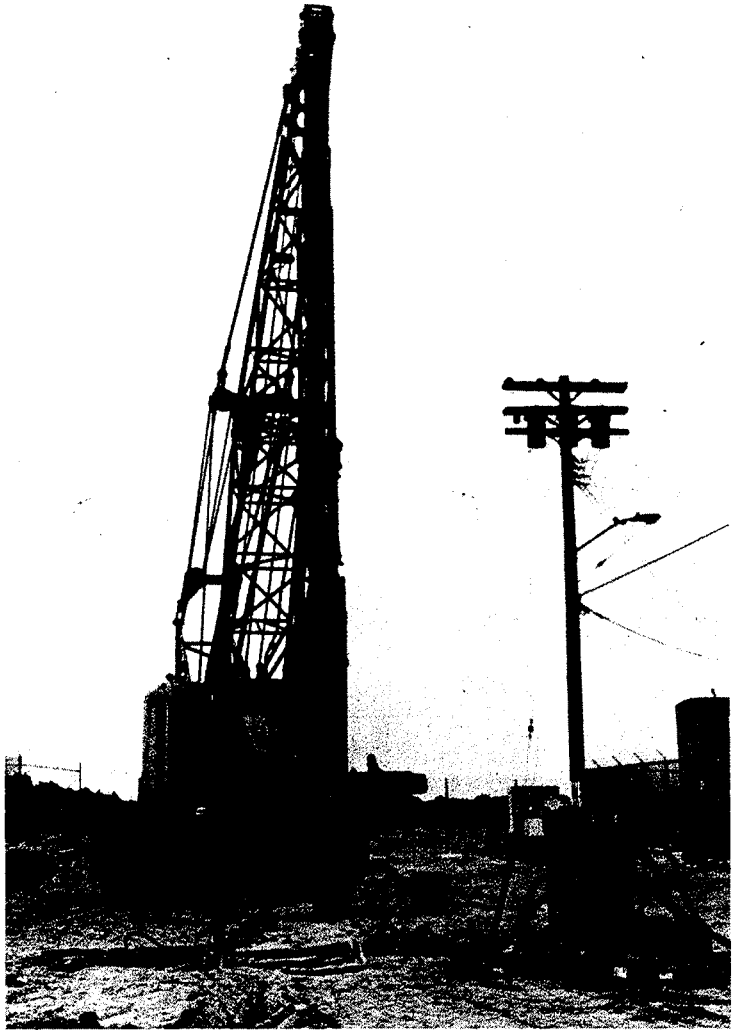

Figure 29. Sheet pile driving test, just prior to drive.

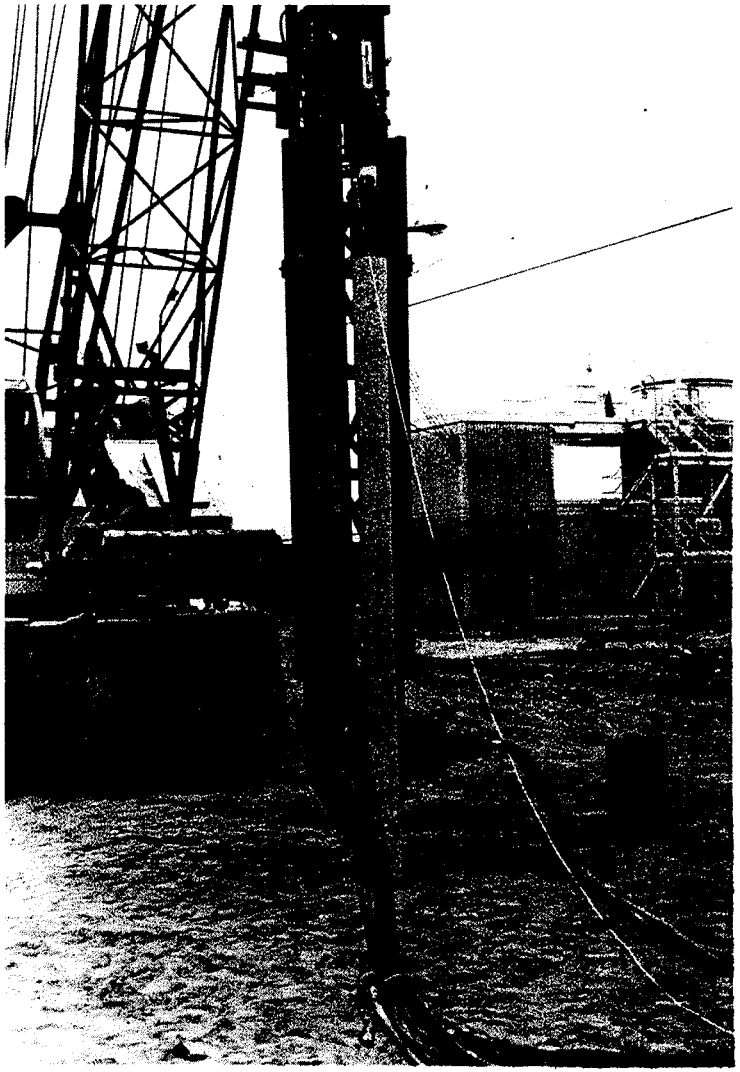

Figure 30. Concrete pile driving test, just prior to drive.

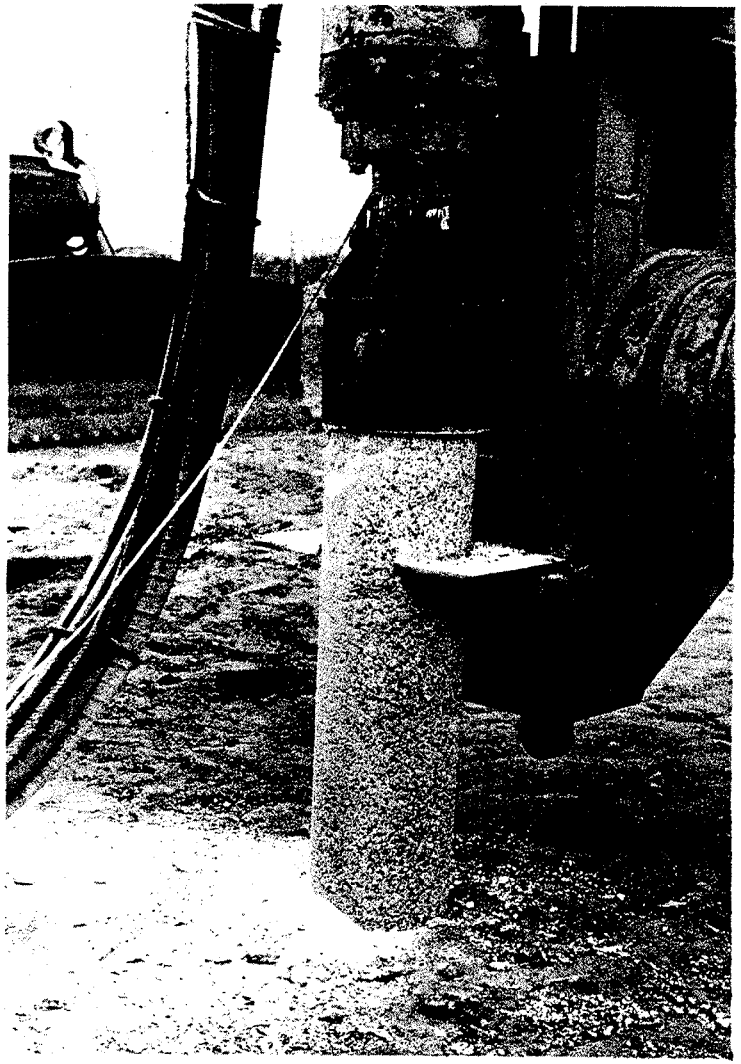

Figure 31. Test drive of concrete lamp post without metal cap.

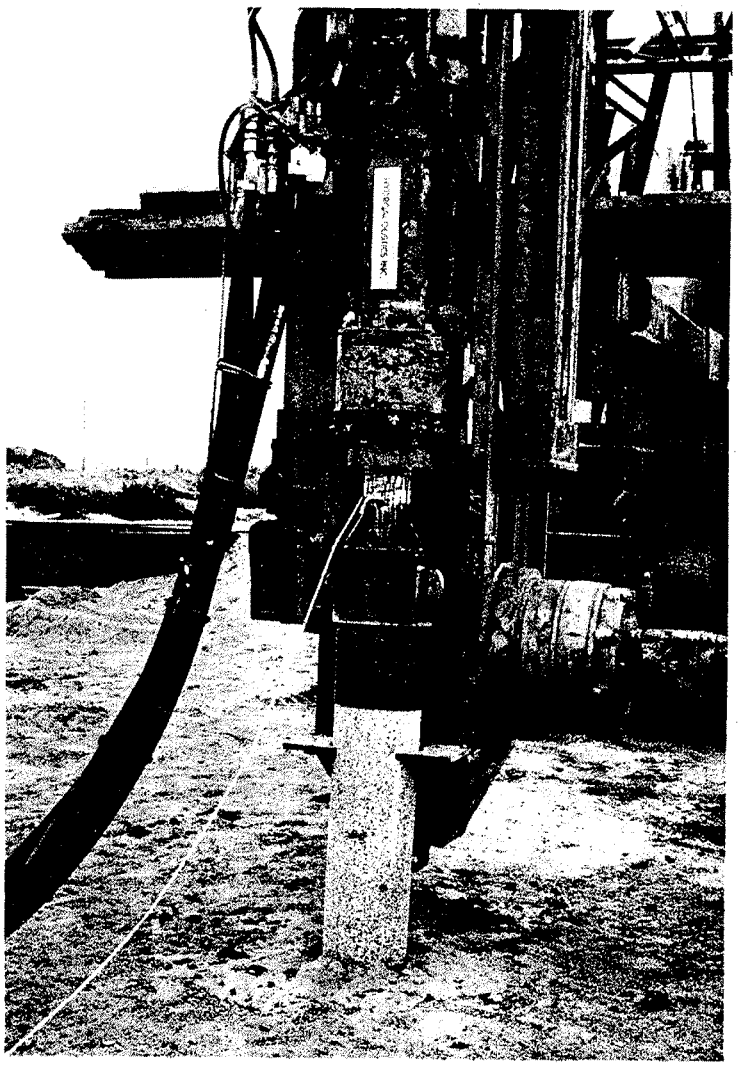

Figure 32. Test drive of concrete lamp post with metal cap.

Figure 33. Underwater test site, empty.

Figure 34. Underwater test site, filled.

REFERENCES

1. "Vibratory pile driver looks good," Western Construction, No. 240, May 1965.

2. Naval Facilities Engineering Command, Chesapeake Division. A Comparison of current and projected methods of driving piles, by A. Rinakli. Washington, D.C., Oct. 1970.

3. Army Corps of Engineers. SR 141: Pile driving by means of longitudinal and torsional vibration, by Austin Kovacs and Frank Michitti. July 1970.

4. Naval Civil Engineering Laboratory. Technical Report R-088: Evaluation of the McKiernan Terry DE20 Diesel Pile Hammer, by J. J. Hromadik. Port Hueneme, CA, 1960.

5. Michigan State Highway Commission. RP 61F-60: A performance investigation of pile driving hammers and piles, by A. W. Ferguson. Lansing, MI, Mar 1965.

6. General Dynamics Corp., Electronics Division. Report No. HL110-69: Comparison of hydroacoustic impact drivers with resonant eccentric weight pile drivers, by B. A. Wise. June 1967.

7.———. Report No. AC117-70: The IMP-M percussion rock drill with independent rotation, by B. A. Wise. Oct. 1970.

8. R. M. Phelan. Dynamics of machinery. New York, McGraw-Hill Book Co., 1967.

9. I. S. Sokolnikoff and R. M. Redheffer. Mathematics of physics and modern engineering. New York, McGraw-Hill Book Co., 1966.

10. W. W. Hagerty and H. J. Place. Engineering mechanics, New York, D. Van Nostrand Co., Inc., 1962.

11. A. S. Vesić. "Investigations of bearing capacity of piles in sand," North American Conference on Deep Foundations, Mexico City, Dec. 1964.

12. Princeton University. Princeton Soil Engineering Research Series No No. 4: The driving of piles by longitudinal vibrations, by W. E. Schmid and H. J. Hill. Princeton, New Jersey, 1966.

13.——— . Princeton Soil Engineering Research Series No. 11: Vibratory pile driving and ultimate penetration, by W. E. Schmid and A. Gharahamani. Princeton, NJ.

14. Moog Servocontrols Inc. Proposal No. ID-64012: Proposal of electro-hydraulic oscillatory hammer for Raymond International, Inc. East Aurora, NY, Sept. 1964.

15. R. K. Bernhard. "Pile-soil interactions during vibro-pile-driving," Journal of Materials, JMLSA, vol. 3, No. 1, 1968, pp. 178-209.

16. M. Senator. ''Vibratory penetration of soils,'' American Society of Mechanical Engineers, 1967 (Paper No. 67-Vibro-24).

17. Naval Civil Engineering Laboratory. Technical Note N-483: Pile driving by vibrations, by R. J. Lowe. Port Hueneme, CA, 1963.

18. D. D. Barkan. ''Foundation engineering and drilling by the vibration method,'' in Proceedings of the Fourth International Conference on Soil Mechanics and Foundation Engineering, London, Vol. 2, 1957, pp 3-7.

19. U. S. Patent No. 2,975,846: Acoustic method and apparatus for driving piles, by A. G. Bodine. Mar. 21, 1961.

20. Army Cold Regions Research and Engineering Laboratory. Vibratory pile driving and coring in permafrost, by R. W. Huck. Hanover, NH, Nov. 1969.

21. B. K. Hough. Basic soils engineering. New York, The Ronald Press Co., 1957.

22. R. E. Olson and K. S. Flaate. ''Pile-driving formulas for friction piles in sand,'' Journal of the Soil Mechanics Foundation Division, Vol. 93, No. SM6, Nov. 1967.

23. W. Kjellman and Y. Liljedahl. ''Device and procedure for loading tests on piles,'' in Royal Swedish Geotechnical Institute Proceedings No. 3, Stockholm, 1951.

24. MKT Corporation. Manual No. 11-65: MKT Corporation operating maintenance parts manual, Dover, NJ.

25. L. B. Foster Company. Catalog 405-7/71: Data on pile drivers and extractors—vibratory, diesel and air/steam. Seven Parkway Center, Pittsburgh, PA.

26. Naval Civil Engineering Laboratory. Technical Note N-1014: A hand tool selection procedure for Navy construction battalions, by B. C. Witherspoon. Port Hueneme, CA, 1969.

DISTRIBUTION LIST

SNDL Code	No. of Activities	Total Copies	
—	1	12	Defense Documentation Center
FKAIC	1	10	Naval Facilities Engineering Command
FKNI	6	6	NAVFAC Engineering Field Divisions
FKN5	9	9	Public Works Centers
FA25	1	1	Public Works Center
—	9	9	RDT&E Liaison Officers at NAVFAC Engineering Field Divisions and Construction Battalion Centers
—	290	290	CEL Special Distribution List No. 8 for persons and activities interested in reports on Mechanical Systems